(NASA-CR-158134) SURFACE DEFORMATION AND ELASTICITY STUDIES IN THE VIRGIN ISLANDS Final Report (Lamont-Doherty Geological Observatory) 87 p HC A05/MF A01 CSCL 08K

N79-18512

Unclas
G3/46 16317

FINAL REPORT

TO THE

NATIONAL AERONAUTICS AND SPACE ADMINISTRATION

ON

GRANT NSG 5072

"Surface Deformation and Elasticity Studies

in the Virgin Islands"

MAY 1979

PRINCIPAL INVESTIGATORS: Roger Bilham
Christopher H. Scholz

Lamont-Doherty Geological Observatory

of Columbia University

Palisades, New York 10964

Introduction

This report describes work made possible by NASA Grant NSG 5072 and consists of four sections. The first section describes tilt and levelling measurements on Anegada, the most northerly of the British Virgin Islands; the second section contains a discussion of sea-level measurements that were initiated in the region and which played a significant role in the development of a network of sea-level monitors now telemetered via satellite from the Alaskan Shumagin Islands. The third part of the report is a brief description of surface deformation measurements in Iceland using equipment and techniques developed by the subject grant. The final part of the report describes the predicted effects of block surface fragmentation in tectonic areas on the measurement of tilt and strain.

Scientific Achievements 1975-1979

In 1975 we applied to NASA for funds to monitor surface deformation in the Virgin Islands seismic gap in order to understand the mode of energy release at this unusual plate boundary. The N.E. corner of the Caribbean is a seismic gap in that a major earthquake has not occurred in historic time although areas to the west and south have experienced major events. It is not well understood tectonically because the sense of plate motion changes between the Leeward Islands and the Virgin Islands from underthrusting to an oblique-slip motion along the Puerto Rico trench. The geodetic measurements we have made agree with the known geological history of the region in that cumulative tilt is not occurring ($< 10^{-6}$ radians/year). We have had no success in identifying transient strain fields that might arise from aseismic slip at the plate boundary, though these may have occurred during instrument down-time, or at levels below the ambient noise. We conclude that the N.E. Caribbean plate boundary is not undergoing cyclic vertical deformation of the type characterized by the Japanese Pacific coast. This is based more upon the lack of uplifted marine terraces than upon geodetic data since a three-year study is a relatively short time to identify secular signals that may extend over centuries. If crustal deformation is occurring we consider it more likely to be transient, elastic and of relatively small amplitude.

During the investigations we examined various modes of crustal deformation based on Japanese data and formed a number of conclusions concerning suitable methods for monitoring tilts and strains on small islands. Our conclusions are summarized in the scientific publications listed below.

During the Caribbean investigations we developed a simple instrument for monitoring sea level and a small recording package for monitoring slowly varying analog data that can operate remotely for more than a year. Versions of these devices have proven ideal for measuring crustal deformation in other areas chosen for special study by Lamont-Doherty Geological Observatory.

Presently we are operating strainmeters near Palmdale, California, water-level monitors on Lake Taho, Nevada, sea-level monitors in Alaska, and fissure extensometers in Iceland using equipment passed on from the Caribbean experiment.

Finally, the grant has enabled us to initiate satellite telemetry from tiltmeters in the Virgin Islands and sea-level monitors in the Shumagin Islands in the Alaska Peninsula. The Alaska sea-level study enables us to monitor, with a one-month delay, deformation precursory to a major earthquake.

Publications

1. Bilham, R., 1977, A sea-level recorder for tectonic studies, Geophys. J. R. astr. Soc., 48, 307-314.

2. Bilham, R., and J. Beavan, 1978, Tilt measurement on a small tropical island, Proc. U.S.G.S. Conference on Measurement of Ground Strain Phenomena Related to Earthquake Prediction, Carmel, September 1978.

3. Bilham, R. G., and R. J. Beavan, 1979, Tilts and strains on crustal blocks, Tectonophysics, in press.

4. Bilham, R., R. Plumb, and J. Beavan, 1979, Design considerations in an ultra stable long baseline tiltmeter - results from a laser tiltmeter, Proc. Conference on Terrestrial and Space Techniques in Earthquake Prediction Research, Strasbourg, September, 1978, Vieweg Verlag Wiesbaden/ FRG.

5. Bilham, R., and J. Beavan, 1979, Satellite telemetry of sea-level data to monitor crustal motions in the Shumagin Islands region of the Aleutian arc, Proc. Conference on Terrestrial and Space Techniques in Earthquake Predicton Research, Strasbourg, September, 1978, Vieweg Verlag Wiesbaden/ FRG.

Technical Reports

Bilham, R., and A. J. Murphy, 1978, Analysis of data from several tiltmeter arrays, Final Report to USGS Contract 14-08-0001-G371 (Describes technological details of satellite telemetry interface, tiltmeter control systems and tiltmeter testing).

Personnel Involved in the Project

The Caribbean investigations were undertaken by John Beavan and Roger Bilham with assistance from Dee Breger, John Horsfall, Andy Murphy, Dick Perry, George Smith, Vernon Soares, Earle Vanterpool, and Will Webster.

John Beavan and Roger Bilham have extended the work to the Shumagin Islands in Alaska and to Iceland with Egill Hauksson.

We thank David Smith, Dick Allenby, and the staff at NASA for their enthusiastic support of the project. Some of the funding was derived from USGS Contract G-371. We thank the people and government of the British Virgin Islands for their generous assistance. Particular thanks are to Permanent Secretary Mr. E. Georges and Captain Ira Smith for their help.

Section 1.

Tilt measurements in the Caribbean

Geodetic levelling measurements

Summary

We are currently operating three borehole tiltmeters on the Caribbean Island of Anegada in the Virgin Islands. Data from these instruments are telemetered via satellite and searched for internal consistency. A precise measure of secular tilt is obtained from a permanent first-order geodetic levelling line that is measured annually. We conclude that long baseline tiltmeters on small tropical islands will give at least one order of magnitude better stability than shallow borehole tiltmeters. This finding has given impetus to our development of a practical long baseline tiltmeter funded by N.S.F. (Plumb et al., 1979).

Tilt Measurements on a Small Tropical Island

ROGER BILHAM AND JOHN BEAVAN

Lamont-Doherty Geological Observatory of Columbia University,

Palisades, New York 10964

ABSTRACT

Tilt measurements have been made on the Caribbean Island of Anegada (18°44'N, 64°25'W) using precision levelling, sea-level measurements and an array of borehole tiltmeters. The tiltmeter measurements after two years of undisturbed operation indicate a tilt rate of approximately a microradian per month, whereas the precision levelling indicates that the island is stable to within a microradian per year (1976-1978). Variations in sea level appear to affect the tiltmeters coherently, although tidal tilts vary significantly over 400 m distances.

INTRODUCTION

There has been much discussion concerning the fidelity of short-baseline tiltmeters installed near the Earth's surface because there are no published results that can be considered totally beyond suspicion. That is, redundancy and duplication of tiltmeters is rare and coherence of tilt signals is frequently poor even over distances of kilometers. Long-term measurements of tilt do not agree with absolute measurements using independent methods such as levelling. Tiltmeters respond to rainfall, changes in subsurface hydrology and surface temperature and it is usually difficult to exclude some or all of these noise sources as a possible source of observed signals.

Moreover, the generation of tilts can occur through the interaction of local elastic inhomogeneity and applied strainfields. Hence, tilt amplitudes and phases can be distorted even if instruments are of adequately good fidelity. These secondary problems cannot be studied systematically without first demonstrating tiltfield coherence.

It was decided, therefore, that six of the Kinemetrics borehole instruments would be installed sufficiently close to each other to examine the wavelengths of surface tilt and that additional, different tiltmeters and measurements would be introduced to provide an independent evaluation of the real tilt of the area.

LOCATION OF THE EXPERIMENT

The experiment was set up on Anegada in the British Virgin Islands (Figure 1). The Virgin Islands have not experienced a major earthquake in the last 500 years of recorded history but there is reason to believe that a major earthquake may be overdue because regions to the west and south have experienced earthquakes with magnitudes greater than 7. An alternative explanation of the gap in significant seismic energy release may be that strain energy is released in the form of creep or as "slow" or "silent" earthquakes with a large component of long-period energy (minutes to days) and relatively little high frequency energy. The installation of strainmeters or tiltmeters was considered to be a possible means to provide an insight into the two alternative tectonic mechanisms or others that might be involved. Anegada was chosen to site the array since it is essentially horizontal, low-lying, and surrounded by a shallow shelf. Approximately four microearthquakes a day are detected by the Lamont-Doherty Caribbean Seismic Network and there is about one magnitude 4 earthquake a month. The residents on Anegada feel one or two earthquakes a year, which appear to be centered about 20 km to the NW of the island.

GEOGRAPHY OF ANEGADA REGION

Anegada Island measures approximately 16 km east-west by 3 km north-south. The central and eastern parts of the island are surfaced by partly recrystallized coral reef, calcarenites and calcareous sand which nowhere attain a height of more than 9 m above mean sea level. The western part of the island is a layer of sand which thickens westward to a maximum of 10 m depth and which rarely exceeds 2 m above sea level except in the form of wind-blown dunes. The western area has a series of salt ponds that drain poorly to the sea. The eastern part of the island consists of interleaved horizontal layers of calcarenite and coral with a vertical spacing of about 1 m between layers. Borehole information does not exist below 20 m.

The island is fringed by coral reefs. To the north the shelf drops steeply toward the Puerto Rico trench and to the east to the Anegada trough. To the south and west the sea floor is uniformly shallow (about 10 m) across to the islands of St. Thomas and Tortolla. Three or four submerged terraces with a vertical spacing of 3-4 m have been identified to the south of Anegada and *Howard* [1970] argues that this signifies stages of geological uplift.

In 1797 Anegada was marked by *Captain Waring* [1797] on a map as the "drowned island" being "almost entirely covered at spring tide". This "drowning" may have referred to the western half of the island which is now at least 50 cm above the highest tide. If we assume that no other process is operating, the difference between Captain Waring's map and the present implies an emergence of approximately 1 to 3 mm/year. A more probable mechanism is that the present surface is the product of sedimentation. The rapid erosion and rebuilding of the westerly tip of Anegada occurs presently during storm conditions although it is clearly restricted by the reef. According to admiralty charts made in 1890 and more recently, shallowing of the sea floor to the south by about 1 m has occurred. This is interpreted as sediment influx and although it is clear that sediment transport from east to west occurs, it is uncertain where such quantities of sand come from.

Studies by *Schomburgk* [1832] and by developers more recently show large quantities of fresh water underlying the island. The general porosity of the island was revealed by two experiments we performed in 1976. A series of wells up to 90 m from the beach at the west end encountered brackish water right up to the beach with a periodic modulation of height caused by the 30 cm sea tide. The amplitude of the periodic effect fell off rapidly to about 30% of the tidal amplitude in the first 10 m and then less than 5% for the next 100 m. A well 1.5 km from the coast shows a 5 cm tide.

TILTMETERS.

In 1976 we installed six Kinemetrics tiltmeters in boreholes in a 2 km array along the island. Our intention was to examine the nature of island tilt noise and the suitability of using borehole tiltmeters in island-arc deformation studies. Operating problems in the first two years of installation encouraged us to reduce the array dimensions to a more modest array of three instruments (numbered 2, 3, and 4 on Figure 4). The details of our initial installation are to be found in the Final Report to USGS contract 14-08-0001-G371. An important feature of the tiltmeter installation is that the tiltmeters were encased in sand-filled

7.5 cm diameter, 3 m long aluminum tubes before being lowered into 15 cm diameter, 3 m auger holes in the coral. The tiltmeter electronics are augmented by a servo-system for maintaining the tiltmeters close to zero output, by a local recording system, and by a centrally located satellite transmitter (DCP). Each installation is covered by a 1 m high mound of white sand canopied by an elevated sheet roof to minimize the direct effects of sun and rain. The installation method successfully reduces thermal contamination of the tilt data to an acceptable level (see Figure 2).

The local chart recorder at each tiltmeter is multiplexed to monitor the x and y tilt channels and the output from a thermistor thermometer positioned within the electronics unit. The chart is advanced at a rate of approximately 5 cm per day. The tilt data are dominated at high frequencies (3-6s) by microseismic tilt that has its origin in surf action on the surrounding reefs. The microseismic noise varies in amplitude from .1 to .3 microradians according to surf conditions. The telemetered data are smoothed with a 20s filter to attenuate the microseismic energy, sampled every six hours on six channels and transmitted twice daily.

During the first two years of operation the signals from the six tiltmeters were greater than 10^{-5} radians per month in random directions. By 1978 the drift rate had reduced to approximately 10^{-6} radians in a month. The observed decay in the drift rate is presumably due to settling of the instrument and may be an elastic adjustment of the borehole tiltmeter casing in response to installation stresses [*Stauder and Morrissey*, 1978].

We present two figures illsutrating recent data. In Figure 2, synchronous data from tiltmeters 2 and 3 are shown. The x and y channels of tiltmeter 2 show a clear semidiurnal tide with a peak-to-peak amplitude of 1-2 microradians. The y channel of tiltmeter 3 shows a diurnal thermal signal with an amplitude of 4 microradians and the x channel suggests a semidiurnal tide with an amplitude of less than 0.5 microradians. The microseismic tilt amplitude is approximately the same amplitude on 2x, 2y, and 3y but is about half that on channel 2x. Three teleseismic earthquakes confirm that the calibration of 2y and 3y are within 20% of each other in that surface wave magnitudes recorded by each are similar. We view the tiltmeter 2 data with suspicion since the tidal amplitudes are larger than we might expect from tidal loading and may be the result of direct influence of semidiurnal variations of hydraulic pressure [*Van der Kamp*, 1973]. Tiltmeter 2 is the deepest operating tiltmeter and is less than 1 m above mean sea level. Curiously, 1976 data from this instrument showed a dominant diurnal thermal variation although its absence in recent data may be the result of an improved surface cover. On the other 5 tiltmeters the maximum semidiurnal tide peak-to-peak amplitude has not exceeded 0.5 microradians. The thermal signal apparent on the tilt data varies in amplitude from 1 to 5 microradians. Much of this signal is the direct effect of temperature on the electronics unit.

In Figure 3 we plot data obtained via satellite between March and July 1978 together with rainfall and sea-level data. Tiltmeter 2 behaves erratically and eventually fails when its negative power line is severed by a goat. Tiltmeters 3 and 4 show an interesting correspondence with sea level. Inflections in tilt and sea level occur at similar times. The sea-level data follow each other for the period plotted but the tiltmeter data have different trends on all channels.

PRECISION SURVEYING

A 2.5 km levelling line was laid out in 1976 consisting of 38 bench-marks in an approximately E-W line along the tiltmeter array. In 1977 the line was extended to the north. Brass levelling pins were cemented into the coral surface at intervals of 40-100 m, although the majority were spaced at 70 m intervals. Cairns were constructed to locate the mid-points of every measurement pair to within 50 cm. We used matched invar rods and a Zeiss Ni2 level with optical micrometer for the measurements. A reading precision of 0.1 mm can be obtained with this equipment.

The levelling line has been measured five times in two years (Figure 4). We adopted standard first-order levelling procedures for the measurements with one addition; where the outgoing and return levelling measurements for an adjacent pair of bench-marks differed by more than 0.3 mm they were repeated the following day. Normally such errors were attributable to a dust particle on one or another of the bench-marks during a previous measurement. The closure errors for the five outward and return levelling runs vary between 0.3 mm and 1.4 mm, that is, within the 1.6 mm error defined as "first order levelling" [e.g., *Bomford*, 1971]. In most cases the errors were less than the ± .6 mm we estimated as the cumulative reading error for the line.

The island tilt tide may be a significant source of systematic error since it has a measured daily peak-to-peak amplitude of up to 2×10^{-6} radians. Surveying was usually done over a period of six hours in the morning and two in the early evening. The whole line was usually surveyed over a period of two days. Consider two extreme possibilities. In a period of six hours the tilt tide could tilt the surface from + 1 μrad to − 1 μrad or it could tilt from zero, ± 1 μrad to zero. In the first instance, a cumulative tilt of 2 μrad would be measured; in the second instance, no tilt would be measured. Note that none of our measurements result in more than a 1 μrad tilt for the whole line but that there are slopes within the line that may be the result of tidal changes of tilt during the measurements. We plan to try to correct the levelling data for the island tilt tide using the borehole tiltmeter measurements.

SEA-LEVEL MEASUREMENTS

A number of measurements of mean sea level are being made on the island and other nearby islands [Figure 1 and *Bilham*, 1977]. On Anegada we are currently operating three sea-level monitors: at the west end, on the NE coast, and in a water well near the center of the island. The latter instrument shows a 5 cm tide and longer period oscillations that closely follow sea-level variations monitored by the other gauges. The two coastal sea-level monitors are installed on the beach and monitor the water table rather than sea level. This experimental arrangement was adopted in order to avoid a direct connection to the sea that we have found vulnerable to vandalism and erosion. The arrangement appears to be effective on Anegada since all three gauges track each other (Figure 3). Long-period changes of sea level are detected by the tiltmeters and can account for some of the inflections in tilt rate observed by the array. Rainfall does not have any obvious effect on either the sea level or tiltmeter data.

DISCUSSION

The tidal tilt of Anegada observed by borehole tiltmeters appears to vary over a relatively short distance (400 m) by a factor of four. The maximum measured value for daily tilt (2 μrad) is sufficiently large to disturb precise geodetic levelling surveys of the island, although the data we present do not appear to be seriously disturbed. This may be due to fortuitous timing of the outward and return surveys used to derive a mean value for the line or it may be due to a systematic error in the tiltmeter measurements. We intend to process the levelling data more carefully to remove the known tilt tide.

An error analysis on the numerical values obtained for each adjacent pair of levelling pins provides a surprisingly low cumulative error estimate; ± 0.6 mm in 2.5 km. This is approximately three times smaller than the maximum permissible error required in normal precision levelling although it has been attained by other investigators [e.g., *Schellens*, 1965]. An earthquake ($M_s = 5$) occurred on 15 Oct. 1976, 20 km to the NW of Anegada. The tiltmeter array was inoperative at the time but the levelling line showed no change ($\pm 2 \times 10^{-7}$) when it was resurveyed nine days later. Over a period of two years there appears to be a suggestion of a tilt up to the NE amounting to 0.5 microradians. Since this value is barely above the estimated measurement precision and we are not yet certain of the influence of tilt tides on the island, we do not place much confidence on its significance.

The long-term tilt rate ($\sim 10^{-6}$ rad/month) seen by the tiltmeters even after two years from installation is approximately an order of magnitude larger than that established by precision levelling. Some inflections in the tilt rate can be accounted for by sea-level variations around and under the island. The levelling data indicate that it may be possible to install a long baseline tiltmeter on the surface between two selected levelling pins to obtain a stability of at least 10^{-6} radians per year. This would represent a significant improvement in the continuous monitoring of surface tilt on the island.

We have observed nothing suggestive of a "slow" earthquake on the data though this may have occurred during the numerous occasions when the tiltmeters were inoperative. The seismograph network operated by this observatory has revealed a complex pattern of earthquakes with magnitudes from -1 to 5 in the Anegada region [*Murphy et al.*, 1978]. Our measurements do not clarify the mechanism of plate collision in this corner of the Caribbean. A longer span of data may help and so would continuous tilt measurements of improved fidelity.

Acknowledgments. We would like to thank the Geophysics Applications Group of NASA, Captain Ira Smith, Earle Vanterpool, and George Anthony Smith for help in various aspects of this study. The work has been supported by USGS contracts 14-08-0001-G286, G290, and G371 and by NASA contract NSG 5072. Linearity tests on the tiltmeters in Ogdensburg Seismic Observatory were made possible by NSF contract EAR 77 04856.

REFERENCES

Bilham, R., A sea-level recorder for tectonic studies, *Geophys. J. Roy. astron. Soc., 48,* 307-314, 1977.

Bilham, R. G., and A. Murphy, Analysis of data from several tiltmeter arrays, *Final Rept.,* USGS contract 14-08-0001-G371, 1978.

Bomford, G., *Geodesy,* pp. 731, Third Edition, Clarendon Press, Oxford, 1971.

Howard, J., Reconnaissance geology of Anegada Island, *Caribbean Res. Inst. Spec. Publ. No. 1,* pp. 1-16, 1970.

Murphy, A. J., W. McCann, and A. Frankel, Anomalous microearthquake activity in the northeast Caribbean: Potential precursors to two moderate-sized earthquakes (abstract), *EOS, Trans. Amer. Geophys. Union, 59,* 8, 1978.

Schellens, D. F., Design and application of automatic levels, *Can. Surveyor, 19,* 2, 1965.

Schomburgk, R. H., Remarks on Anegada, *Roy. Geograph. Soc. Jour., 2,* 152-170, 1832.

Stauder, W., and S. T. Morrissey, Tiltmeter array in New Madrid, *Semi-Annual Tech. Rept. No. 3,* USGS contract 14-08-0001-15848, May 19, 1978.

Van der Kamp, G. S. J. P., Periodic flow of groundwater, *Publ. Ph.D. Thesis,* Free Univ. of Amsterdam, Editions Rodopi N. V., Amsterdam, 1973.

Waring, J., West Indian Atlas, Map of the Virgin Islands, Laurie and Whittle, London, 1797.

FIGURE CAPTIONS

Figure 1. Anegada is the most northerly of the Virgin Islands group. The location of tide gauges and mean sea-level monitors is indicated by a dot.

Figure 2. Copy of typical tiltmeter records from instruments 2 and 3. The tiltmeters were visited on 16 and 19 March 1978 between which times they were minimally insulated from surface temperature variations. The lowest trace on each record is the temperature record. An intermittent fault develops on 2x on 24 March. Teleseismic arrivals are indicated by arrows. A semi-diurnal tide is recorded by tiltmeter 2. Tiltmeter 3 shows a large diurnal thermal signal on the y channel and a small semi-diurnal signal after insulation 19 March on the x channel. The calibration on each record is the same (14 microradians full-scale, 20°C full-scale).

Figure 3. Satellite telemetered data from three tiltmeters. 2x and 2y are disabled by a goat on 30 May and the remaining records are interrupted by the launch of Landsat 4 in late June. The instruments were visited on June 26. The rainfall and daily mean values of sea level are plotted to the beginning of May. Note that inflections of sea level recorded by the three Anegada sea level monitors can be identified on the tiltmeter data. The lowest sea-level trace is obtained from an inland well near the tiltmeters (see Figure 4).

Figure 4. Profile along the Anegada levelling line. The top figure is the topography (vertical exaggeration x 100) with the locations (2-6) of borehole tiltmeters. Data (trace 36 in Figure 3) from a water-level monitor located at position 1 follow mean sea-level data monitored on the coast. The lower figures show the cumulative differences between subsequent levellings and the original (May 1976) levelling.

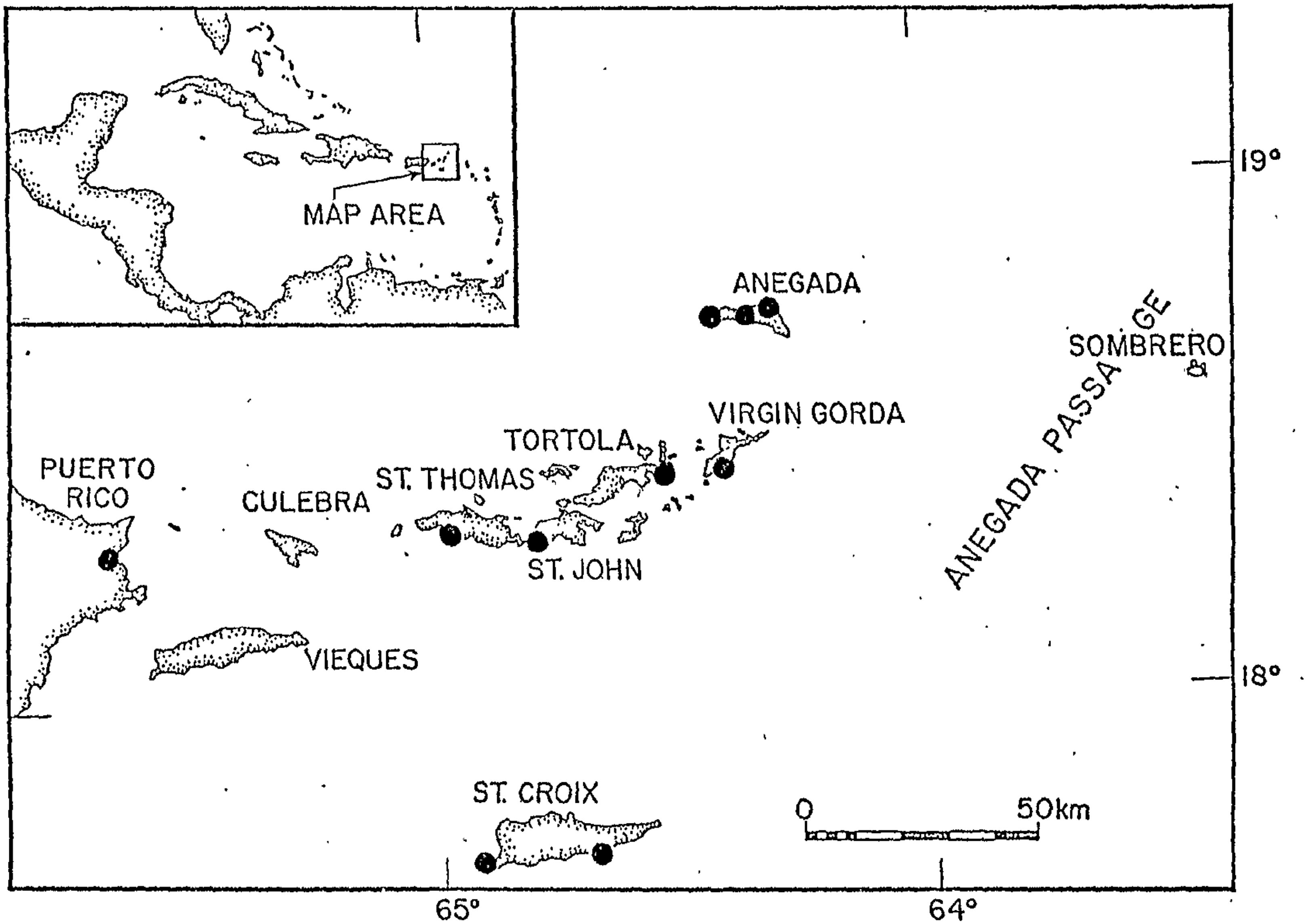
MAP AREA
19°
18°
ANEGADA
SOMBRERO
ANEGADA PASSAGE
VIRGIN GORDA
TORTOLA
PUERTO RICO
CULEBRA
ST. THOMAS
ST. JOHN
VIEQUES
ST. CROIX
0
50km
65°
64°

Figure 1

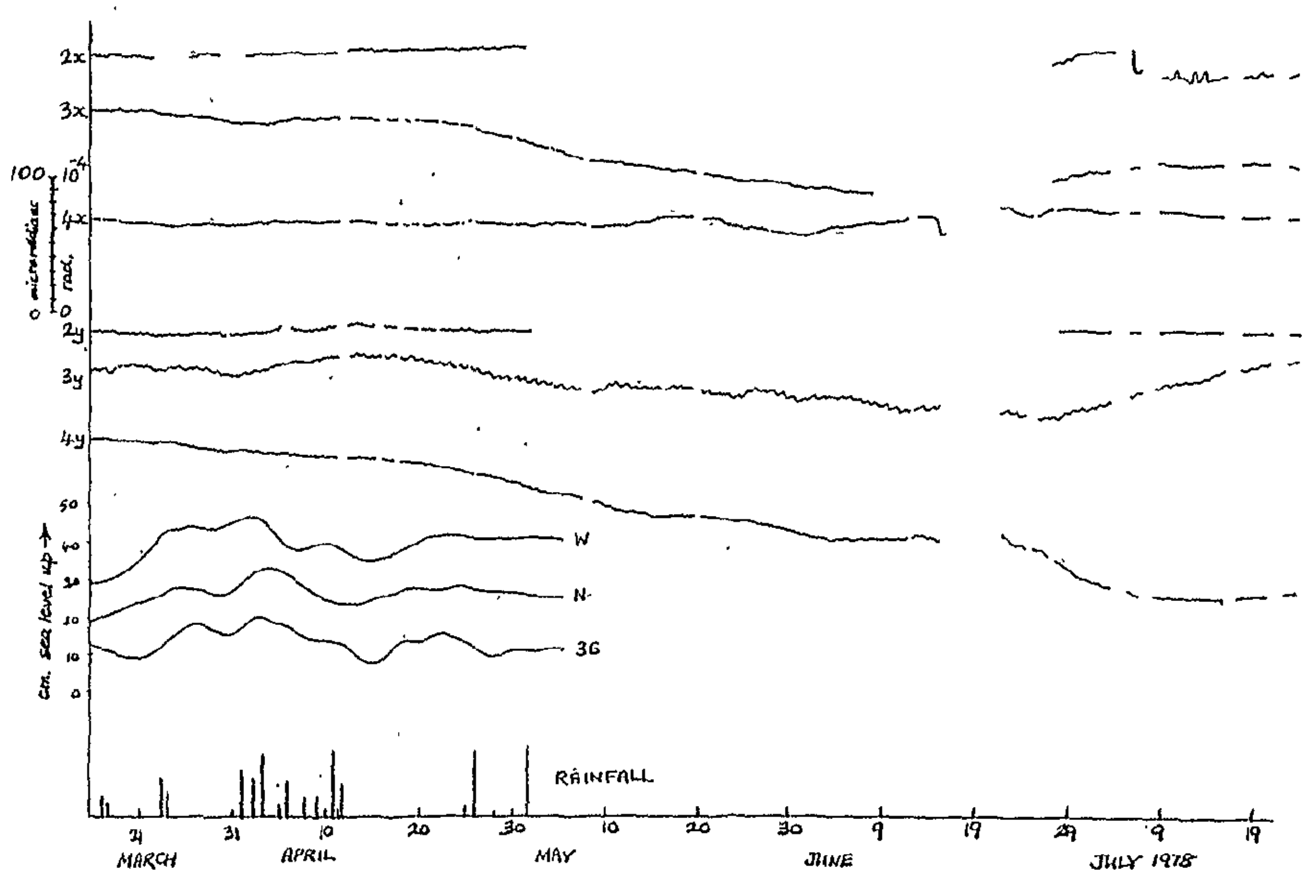
2x
3x
100
10^{-4}
4x
rad.
0
2y
3y
4y
50
40
30
20
10
0
cm. sea level up
W
N
3G
RAINFALL
21
31
10
20
30
10
20
30
9
19
29
9
19
MARCH
APRIL
MAY
JUNE
JULY 1978

Figure 3

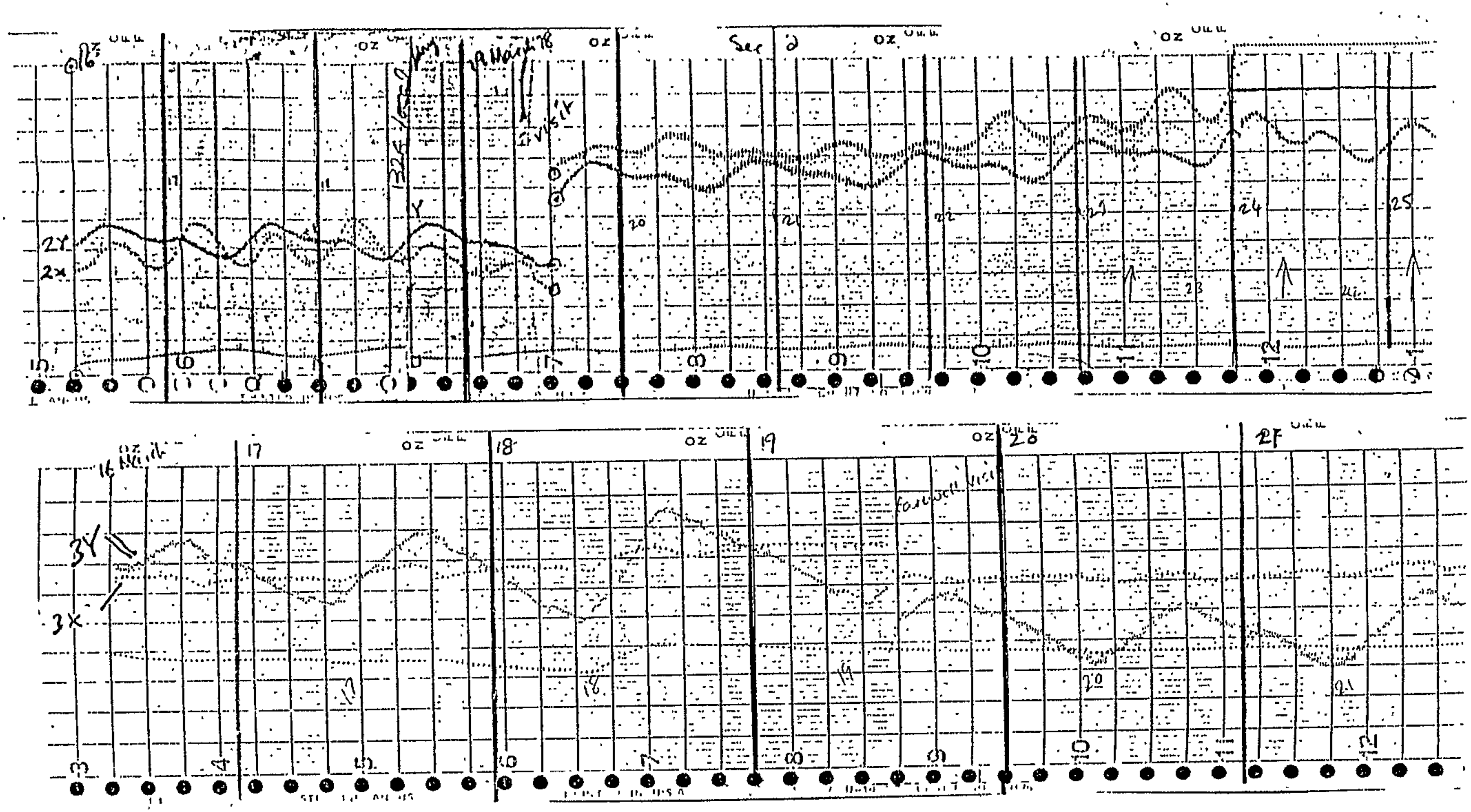

Figure 2

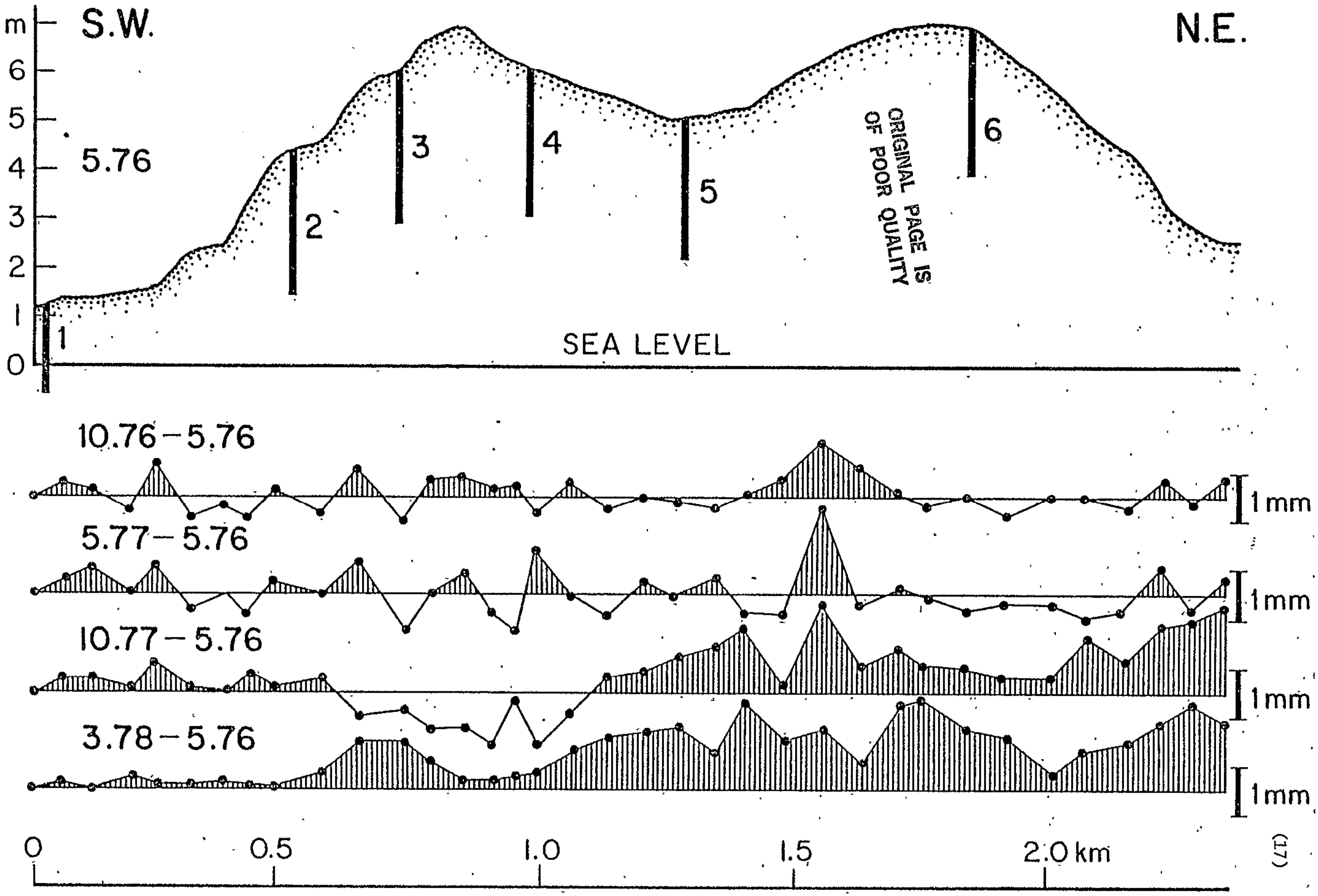
S.W.
N.E.
m
6
5
4
3
2
1
0
5.76
1
2
3
4
5
6
ORIGINAL PAGE IS OF POOR QUALITY
SEA LEVEL
10.76 – 5.76
5.77 – 5.76
10.77 – 5.76
3.78 – 5.76
1mm
1mm
1mm
1mm
0
0.5
1.0
1.5
2.0 km

Figure 4

Section 2.

Measurement of mean sea-level in island arcs

Summary

We have developed a mean sea-level monitor for use on remote coastlines. Currently 15 of these instruments are operating in the Caribbean, Virgin Islands and in the Alaskan Shumagin Islands. The device filters tidal variations of sea level and records the mean value on an analog chart recorder that operates on D-cell batteries for more than a year. Data from the Shumagin Islands are transmitted via satellite and searched for possible relative movements of the islands precursive to a predicted great earthquake.

The development work has provided an insight into coastal hydrology and has identified the need to develop an improved sea-level monitor. The planned design will provide a substantially improved filter characteristic and will also be more adaptable to installation on rocky coastlines (sedimentary beaches are currently used).

Sea-level data from the Virgin Islands do not indicate relative tilt of the islands greater than 10^{-6} radians. Measurements of subsurface water levels on Anegada demonstrate good coherence with sea level except for one gauge on the north coast which appears to sample an inland basin that is charged and discharged in relatively short episodes (Fig. 1).

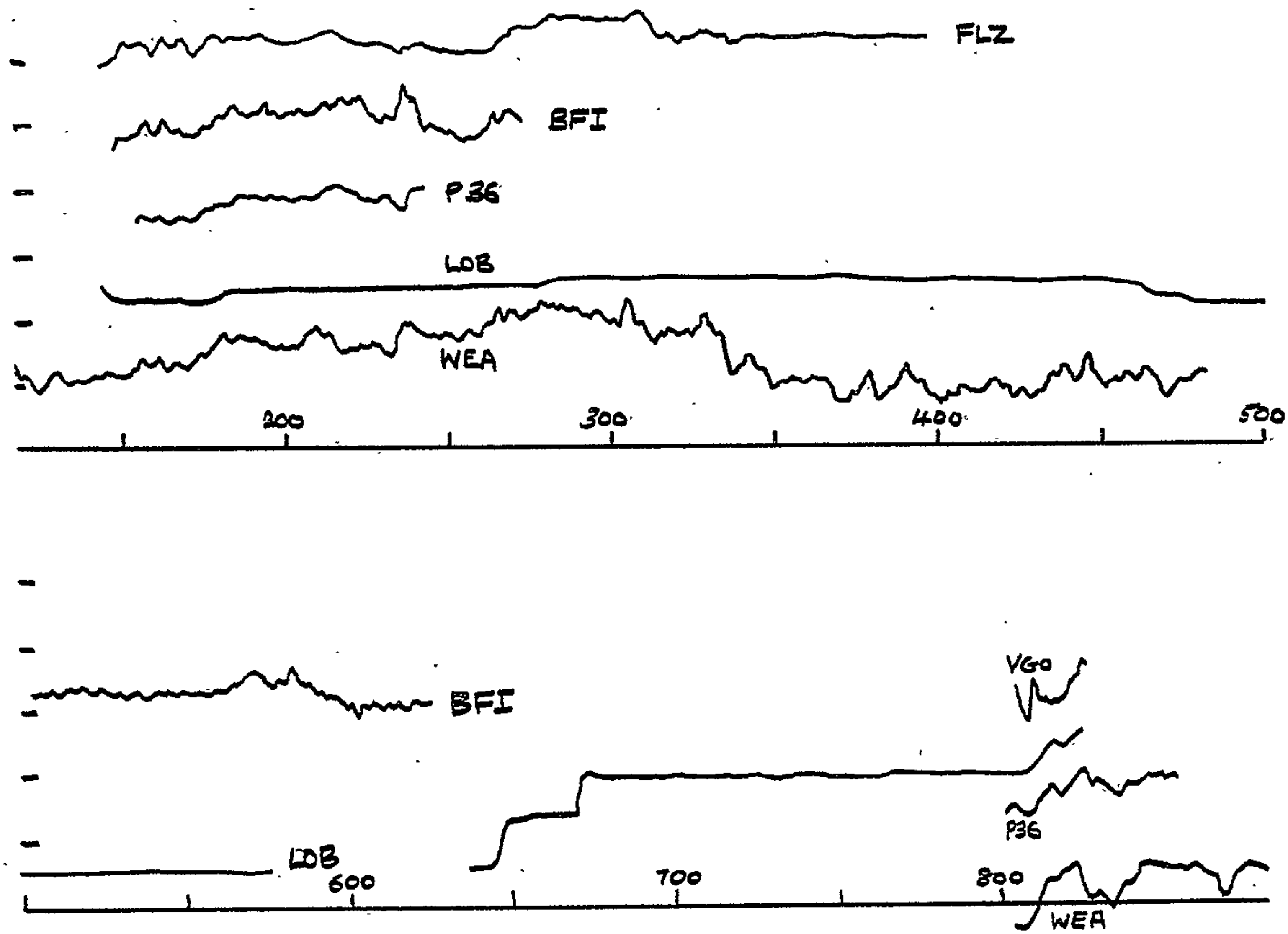

Figure 1. Sea level data from the Virgin Islands. (FLZ = Flamingo Pond, Anegada; BFI = Beef Island, Tortolla; P36 = Central Anegada Levelling Base Bench-Mark No. 36; LOB = North coast Anegada; WEA = West End, Anegada). The horizontal scale is in days from January 1, 1976 and the vertical scale is in 20 cm units. Annual sea-level varies by 20 cm. LOB is poorly coupled to the sea and clearly monitors an inland aquifer. Note that all the Anegada records except LOB track well and that a surge on day 24 is common to the whole network.

Geophys. J. R. astr. Soc. (1977) 48, 307–314

A sea-level recorder for tectonic studies

Roger Bilham *Lamont-Doherty Geological Observatory, Palisades, New York 10964, USA*

Received 1976 September 19; in original form 1976 May 17

Summary. In the past tide gauges have provided valuable information concerning the vertical ground deformation associated with major earthquakes. Although tide-gauge data contains numerous sources of noise; a spacing of less than 40 km between gauges is indicated for a useful study of dilatant behaviour, and a spacing of less than 80 km may be adequate for the study of crustal downwarping in island arcs.

An inexpensive tide gauge is described which is designed to provide a continuous record of sea level with a measurement precision of 1 mm. Hydraulic filtering is incorporated into the instrument in order to attenuate daily tides relative to longer period variations of sea level. The instrument is designed to operate from flashlight batteries for a year unattended and to withstand temporary submersion as might be caused by tsunamis. Several of these sea-level recorders have been installed in seismic gaps in the Aleutians and in the Caribbean.

Introduction

Further progress in earthquake mechanism studies depends in part on acquiring more detailed information on the spatial and temporal distribution of surface deformation in the epicentral region. A traditional source of such data has been tide-gauge records from coastal seismic regions. Careful analysis of existing records shows repeated instances of downwarping and upwelling related to major earthquakes (Omori 1913; Yamaguti 1960; Fitch & Scholz 1971; Scholz 1974; Wyss 1975, 1976). A discouraging feature of many such studies has been the ambiguity present in sea-level data as a result of being unable to distinguish between environmental noise and vertical crustal motions. Environmental noise in tide-gauge data is caused by variations in wind- and sea-current direction, atmospheric pressure and sea temperature and by changes in salinity and global sea level. Using differencing techniques (Tsumura 1971) the effects of some of these variables can be reduced. It is also possible to apply an approximate correction for sea-level variation caused by changes in atmospheric pressure where this has been measured. Using annual means Wyss (1976) concludes that differences in mean sea level between adjacent gauges (~100 km apart) can be established to an accuracy of 1 cm/ Using an array of three gauges over 30 km near Pozzuoli, Italy, Palumbo (private communication) claims a similar precision for monthly means. Although differencing techniques will not be successful in areas where very local variations in sea level may occur, e.g. salinity variations in estuary locations or temperature effects in shallow-shelf seas, in general the denser the array of tide gauges the greater is the noise-suppression capability. In an island arc environment where an archipelago exists it is possible that atmospheric and oceanic variables may contribute less significantly to sea-level variation than they would on an extended linear coastline. Under such conditions an accuracy better than a centimetre may be achieved.

Although present tide-gauge stations are well distributed globally they are frequently too far apart to be of use as recorders of tectonic deformation. Dilatancy diffusion models of earthquake mechanism require surface upwelling in the epicentral region of the order of tens of centimetres (Scholz, Sykes & Aggarwal 1973). For a large earthquake the lateral extent of this deformation may exceed 100 km requiring a tide-gauge spacing of the order of 30 km to ensure adequate coverage. In Japan, an average 100-km spacing of tide gauges gave adequate coverage of the Nankaido 1946 earthquake in which the lateral extent of crustal deformation was approximately 1000 km (Fitch & Scholz 1971). By comparison the present distribution of tide gauges in the Aleutian arc is approximately every 1000 km and in the Caribbean every 150 km.

Since tide-gauge data have been crucial in previous studies of major earthquakes we believe that it is important to install additional instruments in particular areas of seismic risk. Consequently we have designed an instrument which is readily adaptable to existing coastlines, is sufficiently inexpensive to install in large numbers and which requires minimal annual maintenance.

We expect that some of the shortcomings of existing tide-gauge data may be reduced by using the new sea-level recorders which due to their cheapness and relative ease of installation can be installed in numbers that were previously not feasible. For example, changes of sea currents are one of the principal sources of relative variations of sea level between nearby coastal sites. By installing a number of sea-level recorders on opposing coasts of small islands an average sea level for that island can be obtained which is less dependent on seasonal sea current and prevailing wind direction. Optional hydraulic filtering in the instrument enables the suppression of the daily tides relative to longer period sea-level changes if required. The instrument can be operated either as a self-recording device or as a remotely recorded device with the addition of a 40-db dynamic range telemetry link.

The instrument

The sea-level recorder consists of three parts; a vertical standpipe, a long flexible entry tube with an inlet in deep water to provide hydraulic connection with the sea and a pressure-tight measurement package (Fig. 1). The entry tube attenuates rapid fluctuations of sea level and enables the installation of the standpipe in a protected inland environment. A capillary tube can also be inserted in the entry path to attenuate the amplitudes of the daily tides relative to longer period variations. This allows greater measurement precision using analogue chart recorders or FM or digital telemetry of limited dynamic range.

The mathematics of the hydraulically filtered tide gauge have been described in Groves (1965) and Filloux & Groves (1960). The time constant of the syphon is given by

$$\tau = 8\nu l a^2 / r^4 g \text{ s}$$

where ν is the kinematic viscosity of sea water (0.01 cm²/s), g the acceleration due to gravity, l is the length of the entry tube, a the inside radius of the standpipe and r the inside radius of

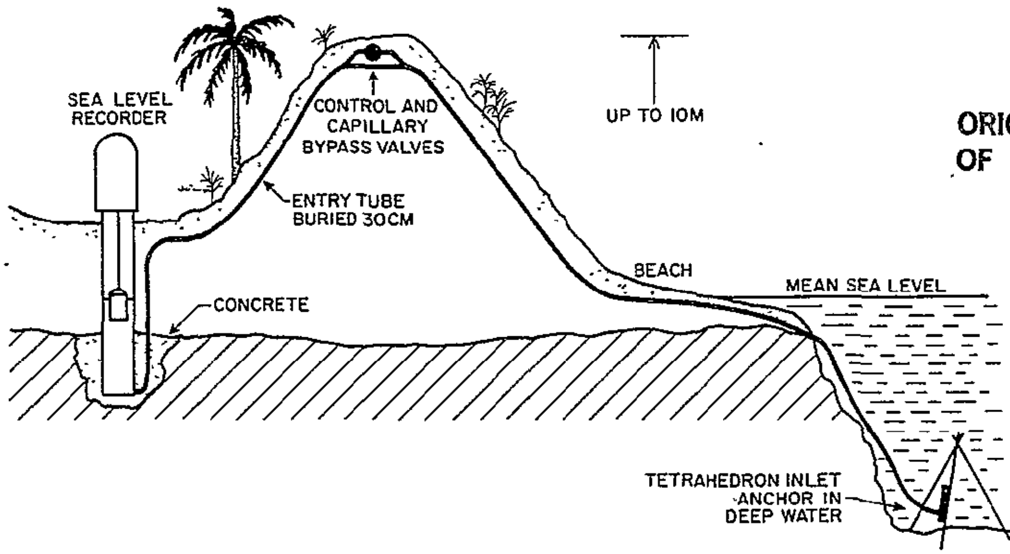

Figure 1. Syphon arrangement of sea-level recorder allows installation on diverse coastlines.

the entry tube. Thus using a 150-m long 6-mm diameter entry tube and an 11-cm diameter standpipe a time constant of approximately 1 hr can be obtained, and by inserting a 1-m long 0.3-mm radius pyrex capillary tube in the hydraulic path the time constant can be increased to about 80 hr. In the Aleutians, where the tidal sea-level variation is approximately 4 m, we chose an 80-hr time constant capillary which led to an attenuation factor of approximately 0.05 for diurnal tides. The resulting diurnal tide was arranged to record as approximately two chart widths using a 10-cm circumference measurement pulley. A 1-hr filter was found to be adequate in the Virgin Islands in the Caribbean where the tide is approximately 30 cm.

The reference float is connected to a counterbalance weight via a wire which passes around a pulley monitored by a potentiometric angular position transducer. Motions of the float appear as a variable voltage which feeds the galvanometer of a chart recorder. The total current consumption of the measurement system varies from 2 to 12 μA depending on the reference float position. Two AAA type alkaline cells are sufficient to operate the sensing system for 18 months (Fig. 2).

The recorder used is a conventional dotting type which uses 6-cm wide waxed pressure-sensitive paper. The recorder motor is operated at 2.8 V for 2 s every 60 s in order to conserve power and prolong motor life. The power is supplied from a single Lithium D-Cell, with a rated capacity of 10 AH. The switching system adopted in the prototype involves a commercial clock movement with a 60 s sweep hand onto which is fitted a pill shaped magnet (6 mm diameter, 3 mm thick, with north–south faces). Each minute this sweeps past a reed relay whose fixed position is adjusted to give the required 2-s contact closure. The clock is operated from a separate battery (1.5 V Alkaline D). The batteries chosen are sufficient to operate the recorder and clock for 18 months. The switching system could employ a solid-state clock with a marginal improvement in power consumption.

Chart speed is adjusted with interchangeable gear boxes. The normal operating time is chosen to be 13 months which gives a chart speed of approximately 5 cm/day.

The electronic calibration depends on the state of the batteries since it is difficult to regulate the low voltage (±1.5 V) in the measurement system without wasting power. How-

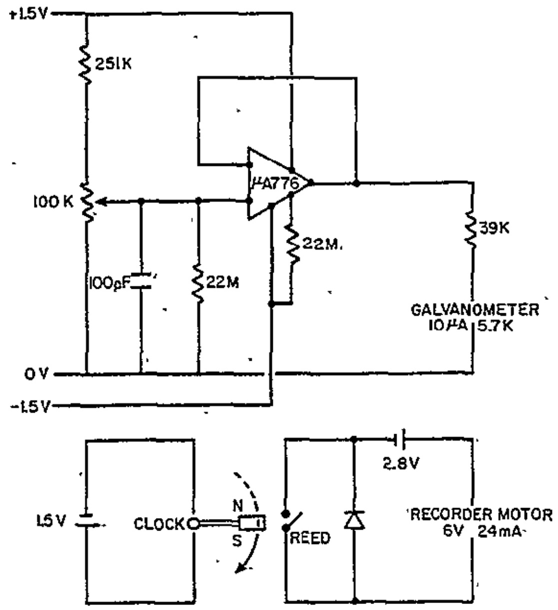

Figure 2. Schematic electronics for tide gauge. Current drain at ±1.5 V is 6 µA average for galvanometer, 600 µA average for clock and recorder motor.

ever, the system automatically calibrates itself as long as the sea level measured oscillates over more than one chart width. For example the sea tides are never removed totally nor are they exactly centred on the chart. Thus as the potentiometer rotates from maximum to minimum or vice versa a record of amplifier calibration is produced (Fig. 6).

Mechanical construction and installation

The base of the standpipe is embedded inland 50 cm below mean sea level in a block of concrete. Bolted to the top of the pipe is the recording/measuring package. The recorder, electronics and batteries are all enclosed in a hermetically sealed PVC tube (Fig. 3). The design is such that during flood conditions, such as could be caused by a high-tide storm or a tsunami, water will be prevented from flooding the electronic compartment even in the event of failure of the O-Ring seal due to the back pressure formed by its bell-shaped geometry. The entire system can thus be flooded to a depth of several metres without damage. This was considered to be a necessary design feature in view of the occasional destruction of Pacific coast tide gauges by tsunamis. The standpipe is installed slightly inland from the coast and is more than 80 per cent buried which further prevents mechanical damage. The measurement system is designed to be replaced annually by a spare unit. This enables rapid inspection in the field and allows careful overhaul of the apparatus in a more favourable environment.

The 150–250-m long entry tube consists of transparent PVC tubing with a 6.3-mm internal diameter and a 12.5-mm external diameter. It is tough and resilient. Air bubbles are easily visible in the tube if it is in air or under water. The entry orifice to the system consists of a 5-cm copper tube approximately 30 cm long, held approximately 1 m above the sea floor by a heavy tetrahedral-shaped anchor. The copper tube discourages barnacle growth and produces a poisonous environment in the entry tube which prevents bacteriological fouling. It points downward so that sediment accumulation cannot occur.

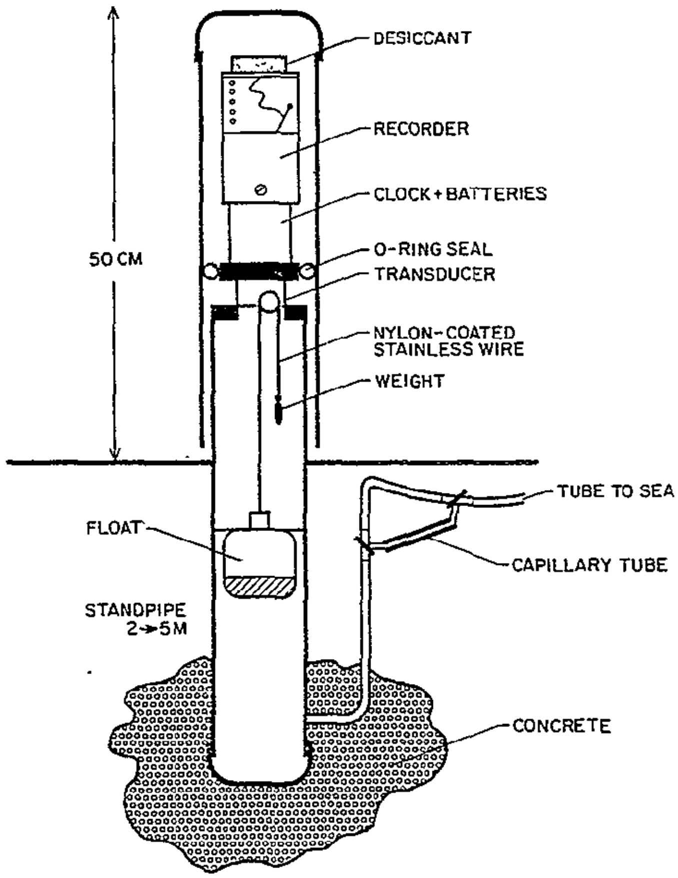

Figure 3. Sea-level recording package. The recorder operates once per minute for a year at approximately 5 cm/day. The sensitivity is determined by the circumference of transducer pulley, normally 10 cm.

The long-term stability of the sea-level recorder is dependent on the standpipe position, the buoyancy of the glass float and frictional effects in the pulley potentiometer. The latter is very low in friction compared to the forces exerted by the float and stainless steel wire (which is wrapped 1.5 times around the pulley). The 10-cm diameter glass float may become heavier if surface bacterial growth occurs and annual inspection will be required to identify such effects. Biological activity within the standpipe is inhibited due to the absence of sunlight. Groves (1965) reports trouble free operation of a remote syphon gauge for many years using a similar system.

The standpipe position is geodetically tied to a nearby solid rock outcrop using a geodetic precision level. Long-term settling of the standpipe is monitored to a precision of 0.2 mm.

The base of the standpipe has to be buried to a depth greater than the lowest expected sea level and the pipe has to be long enough to emerge above the high-water mark. In the Shumagin Islands, Alaska, the tidal range can exceed 4 m so that a 3.3-m standpipe was adopted to ensure its base was below mean sea level. The excavation was carried out by hand to a depth of 3 m at low tide. The resulting hole measured 1.5 x 1 m in area and took two men 4 hr to dig in gravel, sand and soil. Two hundred-pound bags of concrete were mixed with water repellent liquid ('antihydro') and local sand to provide a firm 40-cm deep foundation for the base of the standpipe. The remainder of the hole was filled immediately with the excavated material before the turn of the tide.

The entry tube is buried to a depth of 50 cm under the beach. Ideally this occasion is the lowest low-tide of the month as it was in the case of the Aleutian installations. The tube is more dense than sea water and naturally sinks when offshore. The greatest difficulty arises in burying the tube as it passes under water from the beach. A croquet hoop arrangement was found to be effective in constraining the tube under water on sandy beaches. The Caribbean installations required less excavation due to the much smaller tidal range (30 cm). A 1.8-m standpipe was adopted which could be buried below the low watermark in half a day. Manual excavation in the absence of a large tide is not easy since a major part of the excavation must be carried out under water.

Initially an electric impeller pump was used to fill the system from the seaward end. This introduced cavitation and further installations utilized a hand pump to prevent the production of bubbles. The final adjustment of the syphon was accomplished by operating the valves around the capillary tube. All bubbles were removed by vibration and bleeding the system a few days after installation. Exsolution of air bubbles in the first 24 hr appeared a common feature of the installations.

The tide gauge described fulfils the need for an inexpensive versatile device capable of providing mean sea-level data over periods of years. Instruments have been installed in the Shumagin Islands in the Aleutian Arc and in the Virgin Islands in the Caribbean and further installations are scheduled in these areas to provide an instrument spacing of between 20 km and 60 km (Figs 4 and 5). The two areas are of scientific interest as they are predicted to be the sites of future major earthquakes based on seismic gap theory (Kelleher, Sykes & Oliver 1973). Telemetered seismic monitoring networks are operated by seismologists from Lamont-Doherty in each area.

A short span of tidal data from the Caribbean is presented in Fig. 6. A feature of the record is the automatic scale ranging provided by the angular measurement transducer allowing millimetre resolution of sea level over the entire tidal range. The data can be transmitted in real time using a frequency modulated VHF radio link. The hydraulically

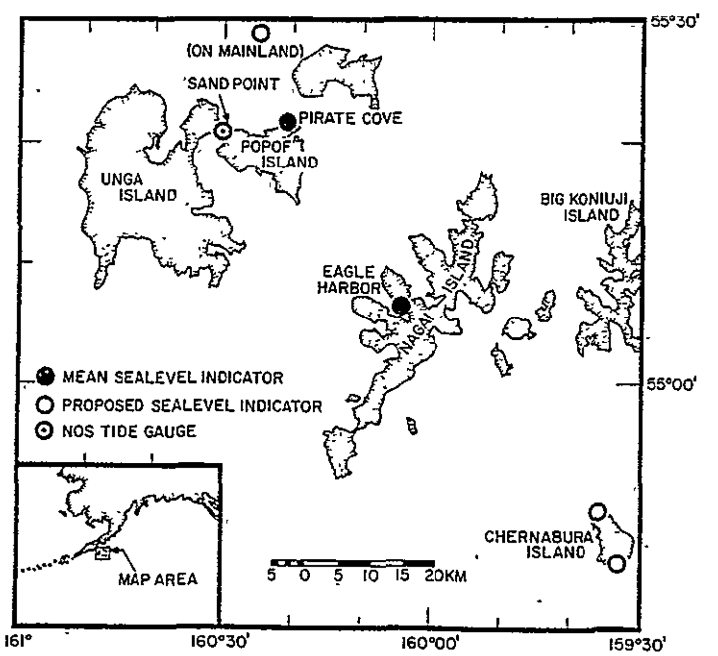

Figure 4. Shumagin Island sea-level recorders. (NOS = National Ocean Survey).

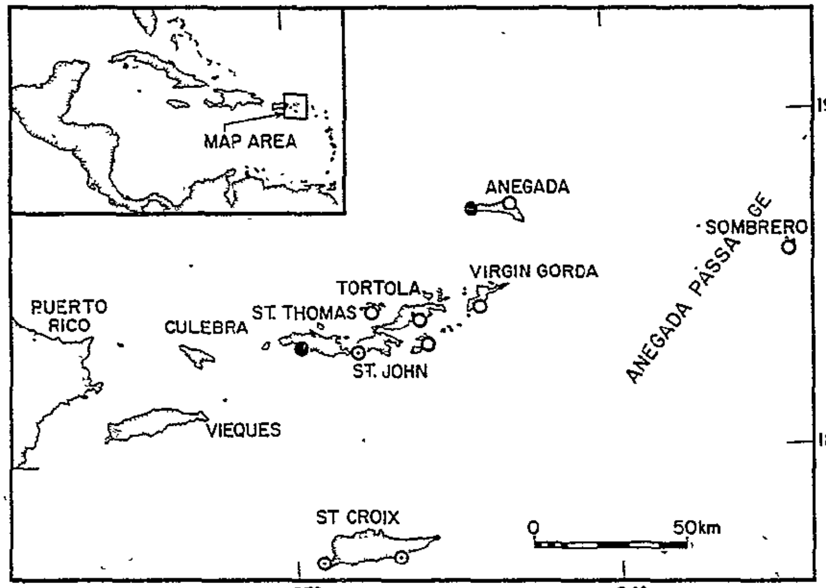

Figure 5. Virgin Island sea-level recorders. Symbols as in Fig 4.

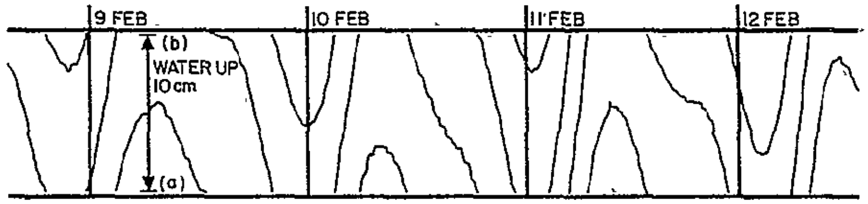

Figure 6. Four days of St Thomas sea-level variation. The hydraulic filtering time constant is approximately 1 hr. Some 60-min seiches are apparent on the records with amplitudes of the order of 3 mm. The angular transducer changes from minimum to maximum output several times during a tidal cycle giving both zero datum and electronic calibration information. Each transducer revolution corresponds to 10 cm.

suppressed tidal output from the tide gauge is suited to digital transmission using satellite relay systems.

An immediate result of the intended dense network of tide gauges in the Caribbean, where the tidal data are recorded virtually unfiltered, will be a more thorough understanding of tidal loading in the region. These data will assist the interpretation of body-tide admittance (Beaumont & Berger 1974) obtained from arrays of tiltmeters installed by Lamont-Doherty on some of the nearby islands.

Acknowledgments

The design and development of the sea-level recorder followed discussions with John Davies, Klaus Jacob, Andrew Murphy and Chris Scholz. Leigh House and Stuart Nishenko installed the two Shumagin Island instruments and provided valuable suggestions for improved performance. My thanks are due to Don Forsyth, Paul Richards and Chris Scholz for critically reviewing the manuscript. The development of the instrument was funded by the National

Aeronautics and Space Administration Grant NSG 5072 and the National Ocean and Atmospheric Administration Grant No. NOAA 03-5-022-70.

Lamont-Doherty Geological Observatory contribution no. 2450.

References

Beaumont, C. & Berger, J., 1974. Earthquake prediction: modification of Earth tide tilts and strains by dilatancy, *Geophys. J. R. astr. Soc.*, **39**, 111.

Filloux, J. & Groves, G., 1960. A seasonal mean sea level indicator, *Deep-Sea Res.*, **7**, 52–61.

Fitch, T. J. & Scholz, C. H., 1971. Mechanism of underthrusting in SW Japan: a model of convergent plate interactions, *J. geophys. Res.*, **76**, 7260.

Groves, G., 1965. Observation of sea level at remote islands, Proc. Symp., *Tidal instrumentation and prediction of tides*, Paris 1965 May 3–7. Pub-Scientifique No. 27, de l'AIOP UNESCO.

Kelleher, J., Sykes L. R. & Oliver, J., 1973. Possible criteria for predicting earthquake locations and their application to major plate boundaries of the Pacific and the Caribbean, *J. geophys. Res.*, **78**, 2547.

Omori, F., 1913. On the recent sea-level variation at the Italian and Austrian mareograph stations and on the cause of the Messina-Reggio earthquake of 1908, *Bull. Imp. earthq. Invest. Comm.*, **5**, 87.

Scholz, C. H., 1974. Post-earthquake dilatancy recovery, *Geology*, 551–554.

Scholz, C. H., Sykes, L. R. & Aggarwal, Y. P., 1973. Earthquake Prediction — a physical basis, *Science*, **181**, 803.

Tsumura, K., 1971. Investigation of mean sea level and its variation along the coast of Japan (Part 2), *J. geodetic Soc. Japan*, **16**, 239.

Wyss, M., 1975. Mean sea level before and after some great strike-slip earthquakes. *Pure appl. Geophys.*, **113**, 107.

Wyss, M., 1976. Local sea level changes before and after the Hyuganada, Japan earthquakes of 1961 and 1968, *J. geophys. Res.*, **81**, 5315.

Yamaguti, S., 1960. On the changes in the heights of mean sea levels before and after the great earthquakes, *Bull. earthq. Res. Inst.*, **38**, 145.

SATELLITE TELEMETRY OF SEA-LEVEL DATA TO MONITOR CRUSTAL MOTIONS IN THE SHUMAGIN ISLANDS REGION OF THE ALEUTIAN ARC

Roger Bilham and John Beavan
Lamont-Doherty Geological Observatory
of Columbia University
Palisades, New York 10964 USA

SUMMARY

Sea level is being used to provide a datum for monitoring vertical tectonic deformation in the Shumagin Islands Seismic Gap. An array of sea-level monitors has been installed that records filtered near-shore sea-level variations and in some cases, piezometric pressures on shorelines with a resolution of 1 mm of water height. The data from the sea-level monitors are transmitted via satellite to provide hourly values for analysis. The spacing between monitors is less than 30 km to enable deformation processes to be studied in detail. In the last two years, the islands have tilted to the south with an amplitude of approximately 10^{-6} radians/year.

Lamont-Doherty Geological Observatory Contribution No. 3787

INTRODUCTION

In this article we describe experimental measurements of mean sea-level to monitor vertical tectonic motions in the Aleutian Shumagin Islands, a seismic gap in the eastern Aleutian Islands arc, Alaska.

Seismic gap theory has proved to be remarkably successful at predicting the approximate location and imminence of future great earthquakes (Kelleher [1], Kelleher _et al_. [2], McCann _et al_. [3]). The method involves assessing the spatial or temporal pattern of energy release historically exhibited by a seismic belt in order to identify regions that appear to be overdue for a major event. The precise location and time of such an event cannot be predicted without additional information describing physical conditions in the source region. A major source of data indicating a relationship between seismicity and crustal deformation has traditionally been the measurement of sea level. Co-seismic deformation is dramatically illustrated in many parts of the world by raised beaches and submerged cities and forests. There are also examples of preseismic and post-seismic movements (Omori [4], Imamura [5], Yamaguti [6], Fitch and Scholz [7], Mescherikov [8], Wyss [9,10], Scholz and Kato [11], Brown _et al_. [12]).

There are two shortcomings to sea-level data when used to study crustal deformation; the distribution of tide gauges is frequently poor and insufficiently dense to provide spatial details of the deformation process, and sea-level has numerous sources of noise that render it far from being the stable geopotential surface that one would like for precise measurements.

Location of sea-level measurements

The present distribution of tide gauges is determined by the oceanographer rather than the seismologist. Thus gauges are placed in locations selected to give useful tidal data over a wide region. Frequently instruments are spaced several hundred km apart or farther if no suitable harbor exists. In seismotectonic studies the minimum desirable density of sea-level monitors is related both to the size of the earthquake and its mechanism. In the present study we are concerned with events greater than $M_w = 7$ (Kanamori [13]) and with rupture lengths greater than 50 km. We assume that surface deformation will be detectable out to several fault lengths and estimate that an instrument spacing of between 10 and 30 km may provide satisfactory details of the deformation process. Thus, in comparison to oceanographic requirements, a denser distribution of instruments is called for and ideally one that is uniformly spaced on the two-dimensional surface overlaying the epicenter. This is rarely possible and even with many more tide gauges most coastlines will represent only a fraction of the surface of interest. Improvements to absolute pressure transducers may enable measurements of sea level in deep-water regions if monitoring and maintenance difficulties can be overcome, but it seems that, at present, conventional gauges offer a practical method in suitably selected areas of interest.

Archipelagos, island arcs and regions with incised or irregular coastlines appear most promising as areas for immediate study. One such region is the Shumagin Islands in the Aleutian arc (Fig. 1). In this region a chain of islands stretches more than 100 km toward the trench from the mainland. The most southerly land mass is approximately 120 km from the deepest point of the trench and seismic studies have shown the Benioff zone to be less than 30 km deep at this southerly point, deepening rapidly northward (Davies and House [14]). The region is identified as a seismic gap and is sited between the 1957 Andreanof-Fox Island earthquake and the 1964 Alaska earthquake, both with magnitudes greater than 8. An earthquake in 1938 may have broken into part of the Shumagin region.

Noise

In tectonic studies any departure of the sea-level surface from the geoid is considered noise. Thus tides are as much noise as are the effects of storm surges, salinity variations, sea-current shifts, atmospheric pressure changes and many more variables that can disturb the sea surface. Relatively few of these noise sources can be removed numerically by measuring the appropriate variable (e.g., atmospheric pressure) and empirical methods designed to compensate for noise

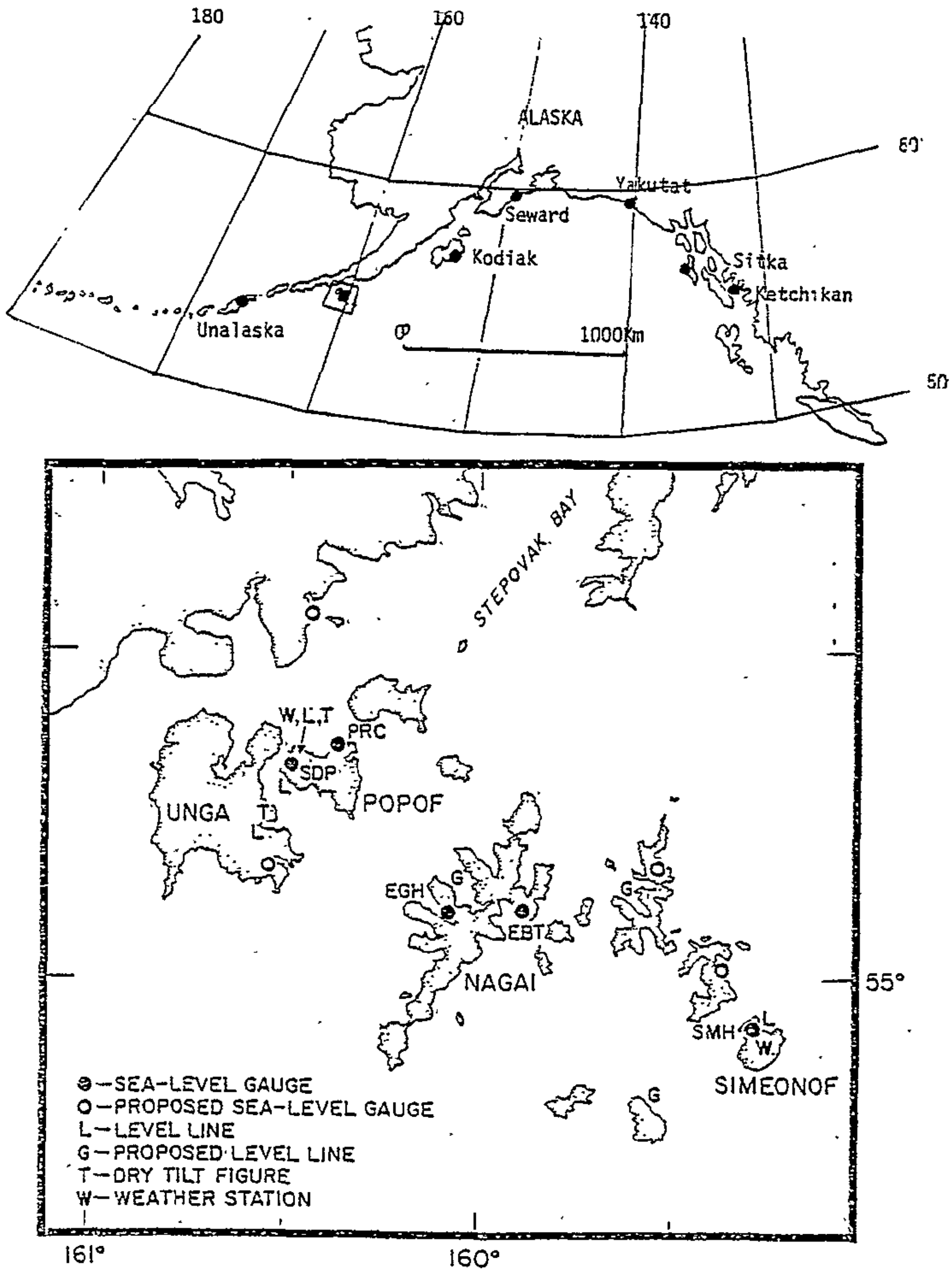

Figure 1. Location of tide gauges and mean sea-level monitors in the Gulf of Alaska and the Shumagin Islands. The region to the west of 163°W experienced a major earthquake in 1957 and the region between 155°W and 145°W broke in 1964. A major earthquake may have partly released strain energy in the eastern Shumagin Islands in 1938 (McCann *et al*. [3]).

can only be partially successful since most of the processes are non-stationary. Fortunately, in a limited area sea-level noise is reasonably uniform. For example, Ingraham _et al_. [15] present analyses of data from the Gulf of Alaska indicating good coherence in sea-level over a wide region (Fig. 2). The annual variation of sea level has a range of 20 ± 5 cm with a minimum in May at six gauges spaced on average 300 km apart. Since we are interested in differences in sea level, i.e., variations in a region less than 200 km in extent, we hope to reduce much of the coherent noise present. We hope to reduce some sources of incoherent noise also by installing more than one instrument on an island. Where possible the sea-level monitors face the sea in opposing directions such that a mean value partially eliminates noise introduced by changes in current direction. A future possibility is that space borne laser altimetry will provide an independent definition of the mean sea-surface. The present accuracy of satellite altimetry is insufficient to be useful (± 10 cm) since present sea-level analysis methods appear to attain 1 cm accuracy even when widely-spaced tide gauges are used (Wyss [9]). Precursory vertical deformation amounting to tens of cm has been reported for some earthquakes (Scholz and Kato [11], Wyss [10]) although there are many examples where any deformation that has occurred is below the noise level of affected tide-gauges. For example, whereas post-seismic deformation is evidently associated with the 1957 Fox Island and 1964 Alaska earthquakes (Fig. 2) there is no obvious precursory sea-level change. Thus the precision desired of a sea-level monitor appears to be of the order of 1 mm. It remains to be seen whether noise sources even in a limited region can be suppressed to this level.

MEAN SEA-LEVEL MONITOR

The sea-level monitor is described by Bilham [16]. The device can be installed on remote coastlines and does not require a jetty or harbor. The system operates from batteries or solar-power and requires a minimum

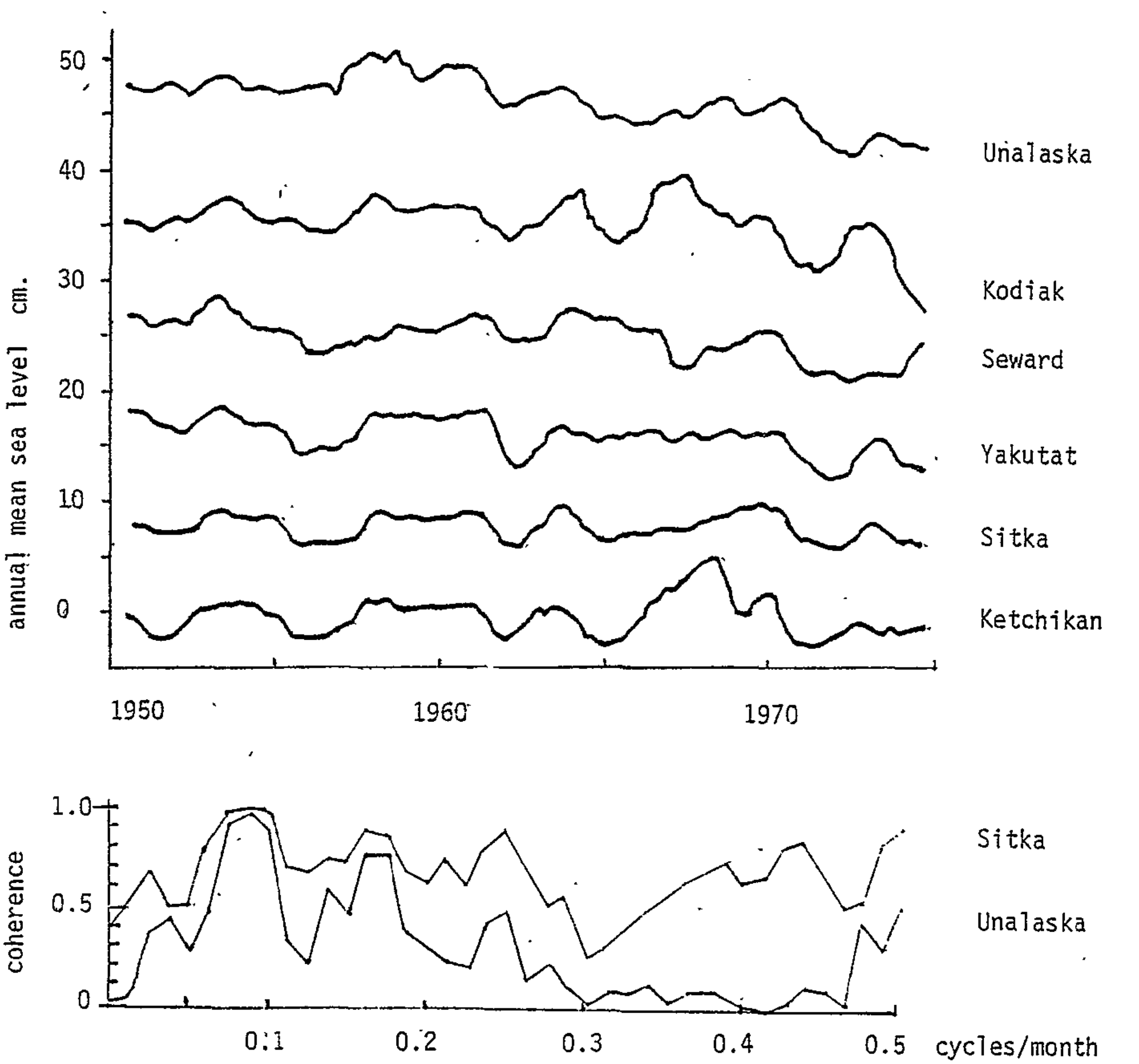

Figure 2. Annual mean sea-level data (1950-1974) from six National Ocean Survey Gauges in the Gulf of Alaska. The data have been smoothed using a 12 month running mean (Ingraham et al. [15]). The Unalaska data after 1957 and the Kodiak data after 1964 show post-seismic land emergence following great earthquakes ($M_s > 8$). The Kodiak and Seward data from 1964 on reflect post-seismic movements that appear also on geodetic levelling data (Brown et al. [12]).

The lower figure shows the coherence for monthly mean sea-level data between Ketchikan and Unalaska, two widely separated gauges (2000 km) and between Ketchikan and Sitka, the closest two gauges (320 km). Coherence clearly falls off with distance though even at 2000 km coherence is shown at annual, semi-annual and ter-annual periods.

of maintenance. It differs from a conventional tide-gauge in that the tides are filtered prior to recording and that it has a resolution of 1 mm in sea-level change. We discuss various problems we have encountered in the operation of the gauge and corresponding improvements to the instrument.

The instrument consists of a vertical tube of about 15 cm diameter buried inland and connected to the sea via a long thin entry tube and a hydraulic filter (Fig. 3). Sea-level variations are monitored in the vertical tube using a float and pulley arrangement. The hydraulic time constant of the gauge is chosen to be large enough to suppress the amplitude of diurnal and semi-diurnal tides to less than 10 cm. Filtering was originally achieved using a length of capillary tubing such that the time constant was given by $\tau = 8\eta\ell a^2 r^{-4} g^{-1}$ seconds where ℓ is the length of capillary tube of radius r cm connected to a standpipe of radius a cm, η is the kinematic viscosity of sea water (sea water = .01 $cm^2 s^{-1}$) and g the acceleration due to gravity. Time constants of the order of 80 hours were found convenient to reduce diurnal tidal amplitudes to approximately 5 cm without attenuating monthly sea-level changes by more than 20%. An alternative method of filtering was to use a porous filter of large area. The 5 cm diameter micropore disc is not clogged by particles of grit in the sea entry tube, which was a problem with the capillary. The micropore filter, typically with a pore size of 0.2 to 0.5 μm, is also sturdier than the capillary but suffers from the disadvantages that it slowly becomes clogged with finely suspended particles so that its time constant increases with time. Fig. 4 shows the percentage amplitude reduction at various periods of sea-level change.

A fundamental problem with the entry tube is that air exsolves from the highly aerated coastal waters and migrates as bubbles to the highest point of the syphon, eventually blocking the tube. Repeated visits were found necessary to evacuate this air and a bubble-trap was devised to extend the useful life of the syphon. This consisted of con-
tainer in the hydraulic line positioned above the topmost of the
syphon (Fig. 3). The tube remains full of water in this nent
until the bubble trap empties. Visits at four-month inte refill
the bubble trap appear to be necessary to maintain syphor ion. The
exsolution of bubbles is not a problem if the entry tube arranged
to incline gently downwards from the base of the standpi s may be
possible with the assistance of earth moving machinery bu mote

Figure 3. (a) Mean sea-level monitor showing hydraulic filtering in entry tube to sea. The entry tube also incorporates a bubble trap to prolong the life of the syphon in the presence of aerated coastal water. (b) Piezometric monitor located on beach. A coarse filter prevents ingress of mud and sand. Variations in the piezometric surface are related to mean sea-level variations, although inland hydrology is a major noise source on many coasts.

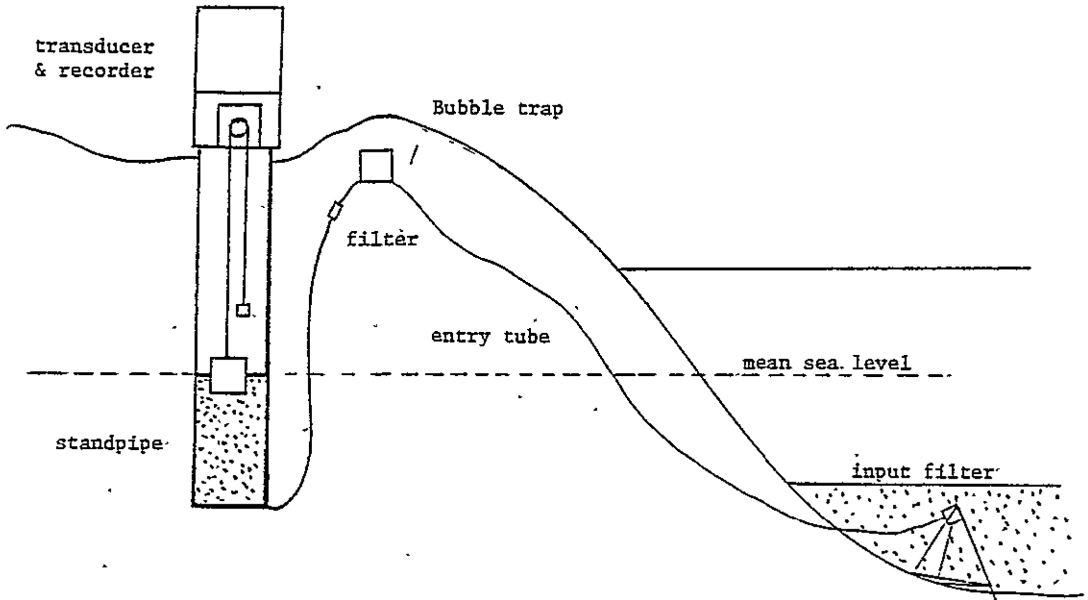

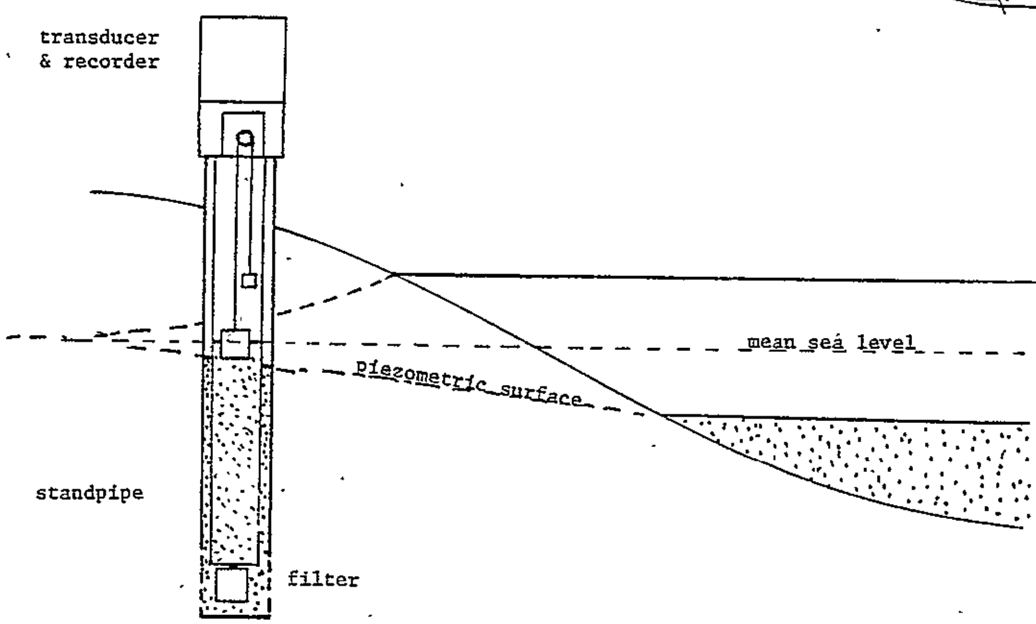

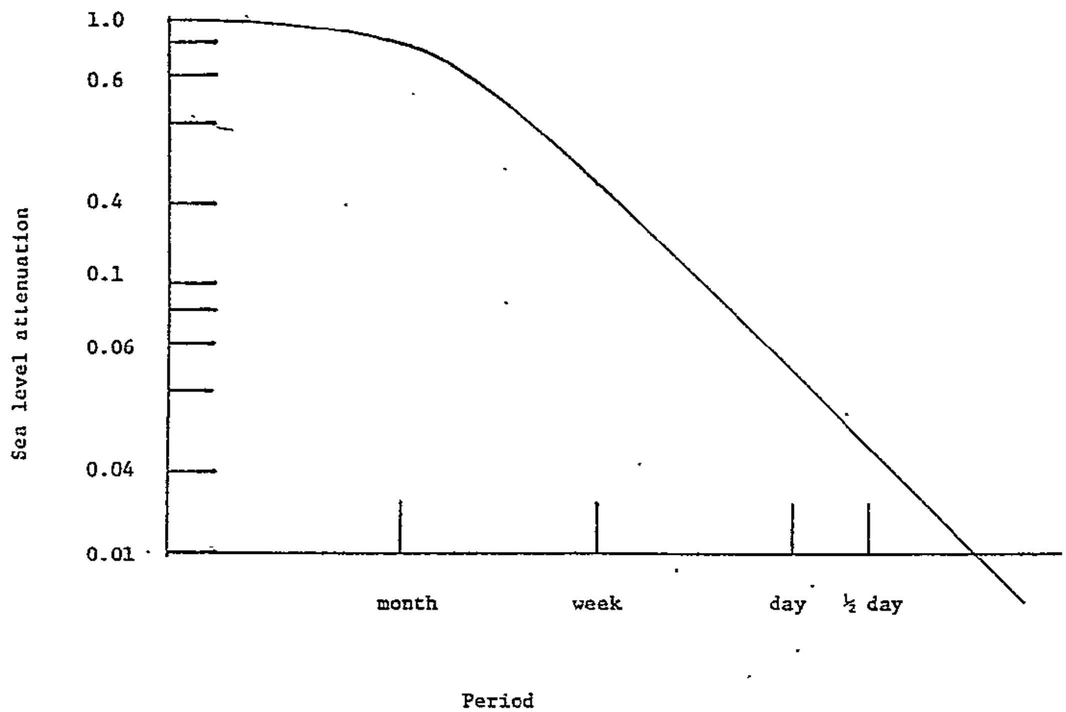

Figure 4. Attenuation of sea level amplitude as a function of period introduced by hydraulic filtering with an 80 hour time constant.

island locations where the installations are invariably by hand it is seldom possible to avoid a syphon arrangement.

An alternative method of avoiding gaseous exsolution in the entry tube is to abandon the direct connection with the sea entirely. This has been tried experimentally in several locations where we monitor water level in a stilling well on the beach. Theoretically, the mean water level in a uniform porous coastal aquifer defines a mean piezometric surface that is equivalent to mean sea level. In practice there are few locations where the piezometric surface is not dominated by inland hydrology. Such is the simplicity of piezometric measurements, however, that we considered it worthwhile to conduct simultaneous measurements of sea level and inland water level to determine their long-term relationship.

Tidal variations in coastal aquifers are caused by pressure variations at the land-sea interface (Van der Kamp [17]). Only at the boundary and a short distance inland does any flow occur. The higher the porosity the slower the decay in tidal variation inland (Fig. 5). During many of our installations we encountered the water table on the beach at approximately mean sea level only metres from the surf. The stability of the water table in some sites is indicated by a marked change in the soil chemistry, from an oxidizing to a reducing environment, a change that occurs over a few cm near the water table (e.g., Pirate Cove, Popof Island). In other sites of higher porosity, e.g., on a gravel spit at Eagle Harbor, Nagai Island the tide was so well-coupled that the underground water-table dropped well below mean sea-level on the outgoing tide.

The mean piezometric water-level inland in a porous aquifer is higher than sea level primarily due to rainfall raising the piezometric surface. The elevation is caused by a "steady-state" fresh water lens in equilibrium with the surrounding higher density sea water and secondly by a transient additional amount of water resulting from recent rain. Both effects can be reduced by choosing a small landmass to undertake measurements (Fig. 6). Alternatively spits of land, narrow headlands, and sand bars have the necessary properties unless they are impounding fresh water (e.g., storm beaches) or near river estuaries. The maximum elevation of the piezometric surface by fresh water is approximately 0.03 of the depression of the saline boundary. If we assume that the fresh water lens is unstable in the presence of sea currents if its depth is more than one third its width, then the fresh water elevation error can be estimated to be approximately 3 cm at the center of a 30 m wide spit. If measurements are conducted near the edge of the spit and an allowance is made for partial contamination of the fresh water, the static error reduces to less than 1 cm. The stability of the lens of fresh water over periods of several weeks and longer is of fundamental importance if the measurements are to reflect sea-level variations, and since this will be unknown at most locations it appears advisable to locate piezometric gauges close to the beach where variations are less significant.

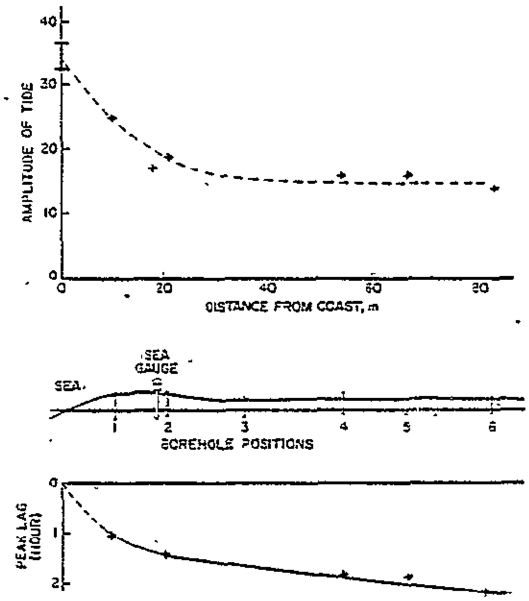

Figure 5. Phase and amplitude relationship observed at various distances inland on a porous sand deposit, West End, Anegada.

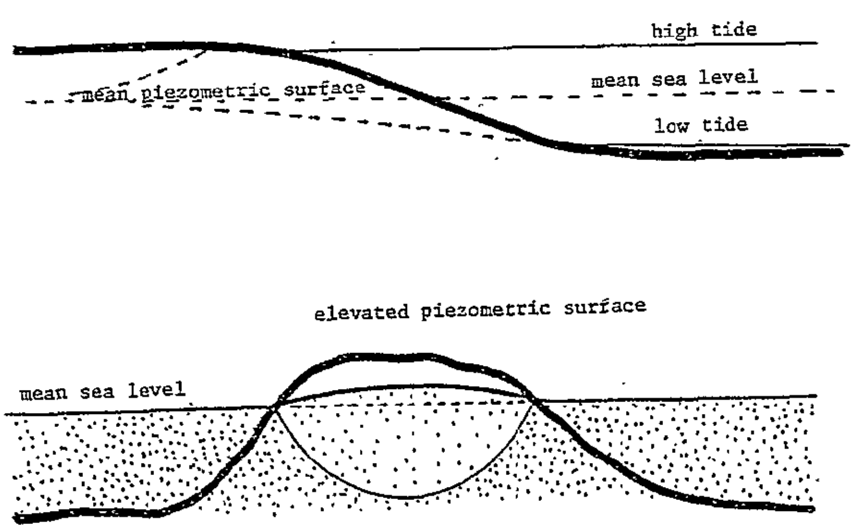

Figure 6. Upper figure: hydrological conditions at a porous boundary in the presence of tides. Flow occurs only in the region near the sea; inland effects are principally fluid pressure changes. Lower figure: the fresh water lens beneath a small island.

DATA RECORDING AND SATELLITE TRANSMISSION

Sea-level data are recorded locally along with air temperature on a strip chart recorder driven by a quartz clock. The angular-position transducer that records the standpipe, fluid-level also provides a 0-5V output that is taken to a LaBarge data collection platform (DCP). The signal is stored in a memory that updates every few hours but which is transmitted in its entirety every 90s using an omnidirectional 400 MHz antenna. At times when the Landsat 3 satellite can see both the DCP and either the Gilmore or Goldstone tracking station, data are relayed to the Goddard Space Flight Center, Maryland. Once a week the data from the entire array of sea-level monitors are forwarded by mail to Lamont-Doherty for analysis.

A sample of satellite data is shown in Fig. 7. Although the Landsat is in polar orbit and therefore can "see" the Shumagins almost every hour, on some passes the sea-level monitors are obscured by mountainous terrain near the site. The lost data are not important and could be reduced either by raising the antenna position or by selecting sites with lower horizons. Alternatively the DCP's can be programmed to transmit to the geostationary GOES satellite in locations with a southerly horizon.

The DCP operates on solar power and can send eight, eight-bit words per transmission in addition to station identification information. Typically the Landsat satellite relays two or three transmissions during its traverse from horizon to horizon, hence it is possible to double the information transmitted from each site. Routinely we transmit the battery voltage level in addition to sea level and/or piezometric level from each site. The benefits of satellite transmission are twofold: we are able to receive data from a remote network of islands with a minimal delay and we are able to monitor instrument malfunction. The second of these has proved to be invaluable in planning field maintenance trips. The Shumagin Islands are difficult to visit due to the exceptionally bad weather common in this part of Alaska. Many sites can be

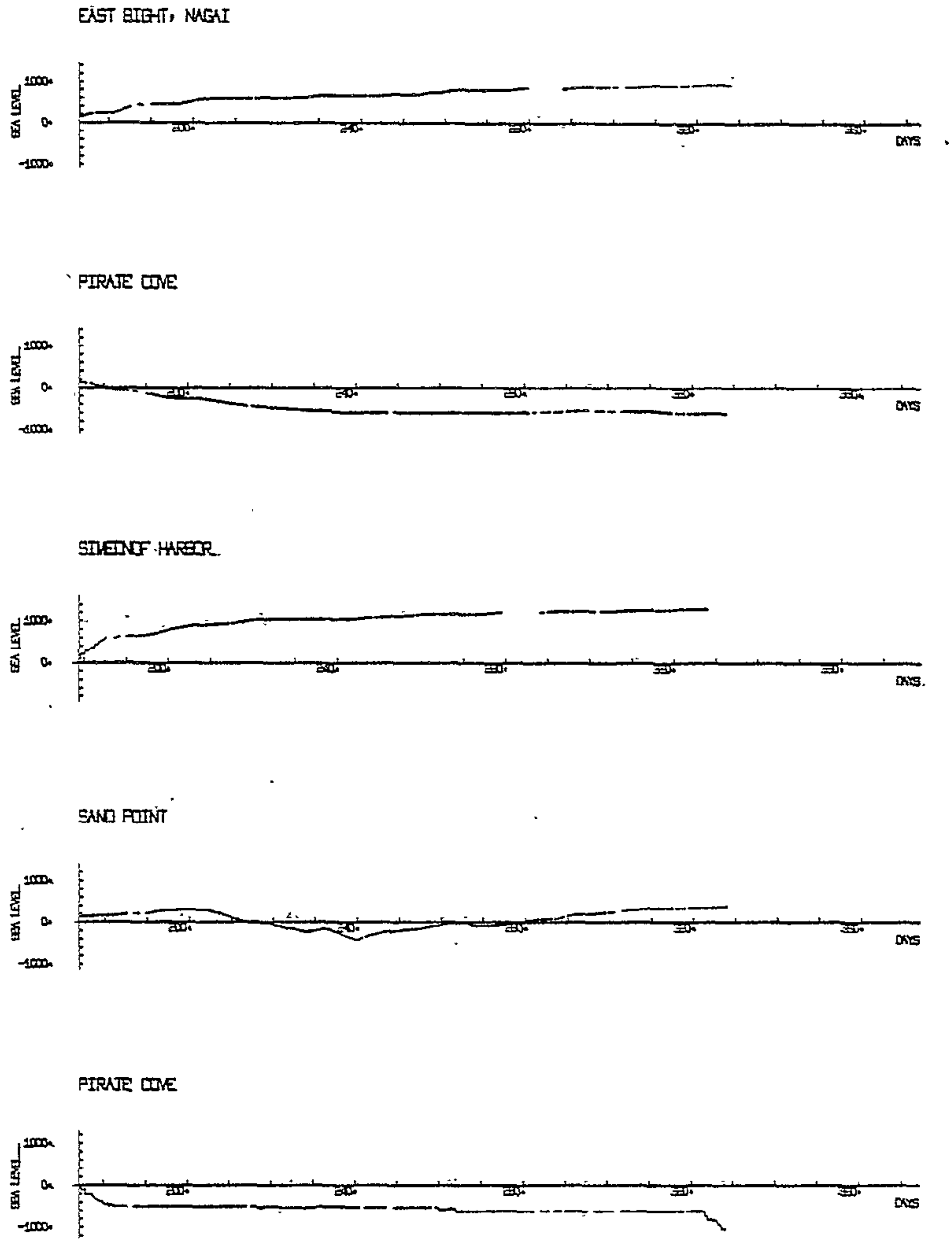

Figure 7. Sea-level data received via satellite from four locations in the Shumagin Islands between July and December 1978. The instruments have hydraulic time-constants of approximately 200 hours. The lower two records are from piezometric monitors. On the lowest record the gauge was malfunctioning from soon after installation until day 322 when it was visited. The vertical scale on these plots is 1000 units equals 40 cm.

visited routinely only once per year and at great expense. A malfunction in a gauge can result in a data gap of many months and may jeopardize the entire experiment. The weekly data provide an immediate check on the number of gauges operating and corrective measures can be initiated when appropriate.

The delay in the data reception caused by mailing time is not critical and can be bypassed if more rapid data transmission is required. We have not considered this to be necessary since the sea-level monitors have time-constants of approximately 3 days and the tectonic precursors we seek extend over months.

DATA

In 1976 we installed two preliminary gauges. These were incorporated into a network of five in 1977 and in 1978 satellite transmission and piezometric measurements were added. Atmospheric pressure is monitored on Popof Island and Simeonof Island. In Fig. 8 we show data obtained in 1977 from these two islands. The two gauges on Popof Island track each other reasonably well but the gauge on Simeonof diverges and apparently indicates a tilt to the south of several microradians. This is consistent with levelling measurements made on two level lines near Popof Island and is typical of the downwarping shown at underthrust plate margins prior to seismic slip (Scholz and Kato [11]). In Fig. 7 we present data collected since the satellite relay was initiated.

CONCLUSIONS

The measurement of hydraulically-filtered sea-level variations is potentially capable of monitoring vertical tectonic motions in island arcs. While we have insufficient data presently to determine the accuracy of our measurements, it is probable that monthly mean values will be accurate to within 5 mm. This corresponds to better than 10^{-7} radians tilt precision across the Shumagin Islands. Long-term comparisons be-

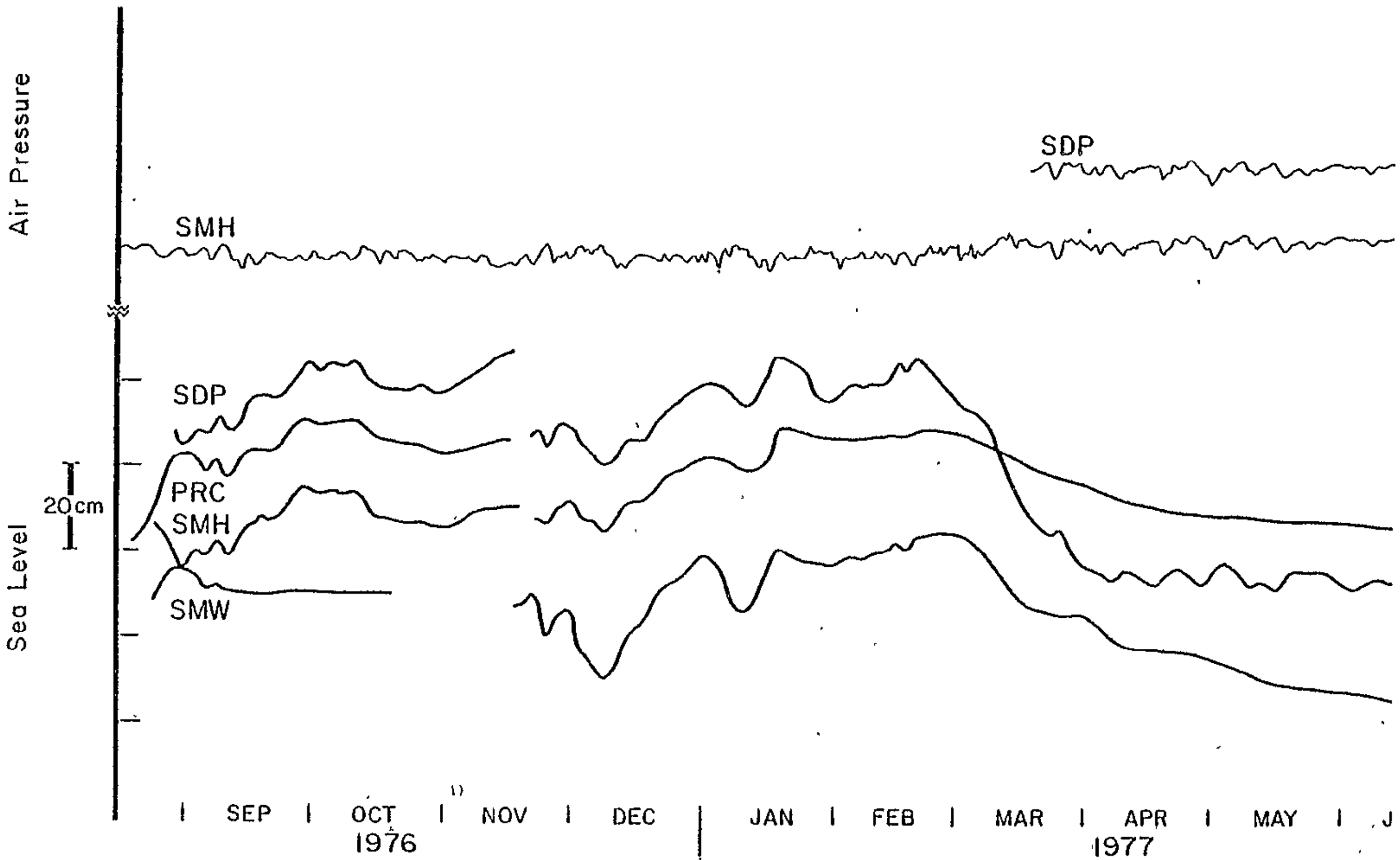

Air Pressure
SDP
SMH
SDP
20cm
PRC
SMH
SMW
Sea Level
SEP
OCT
NOV
DEC
JAN
FEB
MAR
APR
MAY
J
1976
1977

Figure 8

tween shoreline piezometric measurements and sea level are being conducted to determine if simpler instruments may be possible for future work. The use of satellites to relay data for immediate analysis and to check instrument performance makes the operation of a remote network more reliable than was hitherto possible. During the next decade a major earthquake may occur in or near the Shumagin Islands. The ability to monitor surface deformation continuously and remotely through the preseismic and post-seismic stages is an exciting advance in tectonic studies.

Acknowledgments

The work has been funded by the National Oceanographic and Atmospheric Administration (NOAA 70), the Department of Energy (ERDA EY-76-S-02-3134), and the National Aeronautical and Space Administration (NSG 5072). The satellite DCP's are on loan to us from the Geophysics Applications Branch of NASA and we gratefully acknowledge the assistance of Dick Allenby, Gil Meade and Will Webster who have helped organise the satellite telemetry. We thank John Davies and Chris Scholz for their comments on the manuscript.

REFERENCES

[1] Kelleher, J. A., Space time seismicity of the Alaska-Aleutian seismic zone, J. Geophys. Res., 75, 5745-5756, 1970.

[2] Kelleher, J., J. Savino, H. Rowlett, and W. McCann, Why and where great earthquakes occur along island arcs, J. Geophys. Res., 80, 260-271, 1975.

[3] McCann, W., S. P. Nishenko, L. R. Sykes, and J. Krause, Seismic gaps and plate tectonics: seismic potential for major plate boundaries, USGS Open File Report 78-943, 441-584, 1978.

[4] Omori, F., On the recent sea level variation at the Italian and Austrian mareograph stations and the cause of the Messina-Reggio earthquake of 1908, Bull. Imp. Earthq. Invest. Comm., 5, 87, 1913.

[5] Imamura, A., On crustal deformations preceding earthquakes, Jap. J. astr. Geophys., 10, 82-92, 1933.

[6] Yamaguti, S., On the changes in the heights of yearly mean sea-levels preceding the great earthquakes, Bull. Earthq. Res. Inst., Tokyo Univ., 46, 1269, 1968.

[7] Fitch, T. J., and C. H. Scholz, Mechanism of underthrusting in SW Japan: a model of convergent plate interactions, J. Geophys. Res., 76, 29, 7260-7292, 1971.

[8] Mescherikov, J. A., Recent crustal movements in seismic regions: geodetic and geomorphic data, Tectonophysics, 6, 29-39, 1968.

[9] Wyss, M., Mean sea-level before and after some great strike-slip earthquakes, Pure Appl. Geophys., 113, 107, 1975.

[10] Wyss, M., Local sea-level changes before and after the Hyaganada, Japan earthquakes of 1961 and 1968, J. Geophys. Res., 81, 5315, 1976.

[11] Scholz, C. H., and T. Kato, The behavior of a convergent plate boundary: crustal deformation in the South Kanto District, Japan, J. Geophys. Res., 83, 783-797, 1978.

[12] Brown, L. D., R. E. Reilinger, S. R. Holdahl, and E. I. Balazs, Postseismic crustal uplift near Anchorage, Alaska, J. Geophys. Res., 82, 3369-3378, 1978.

[13] Kanamori, H., The energy release in great earthquakes, J. Geophys. Res., 82, 2981-2988, 1977.

[14] Davies, J. N., and L. House, Aleutian subduction zone seismicity, volcano trench separation and their relation to great thrust type earthquakes, J. Geophys. Res., in press, 1979.

[15] Ingraham, W. J., A. Bakun, and F. Favorite, Physical oceanography of the Gulf of Alaska, Final Report RU-357. Environmental Assessment of the Alaskan Shelf, U. S. Dept. Interior, Bureau Land Management, July 1976.

[16] Bilham, R., A sea-level recorder for tectonic studies, Geophys. J. R. astr. Soc., 48, 307-314, 1977.

[17] Van der Kamp, G. S. J. P., Periodic Flow of Groundwater, [Publ. Ph.D. Thesis], Free Univ. Amsterdam, Editions Rodopi N.V., Amsterdam, 1973.

Section 3

Extensometer measurements

of a rifting episode in northern Iceland

Summary

The sea-level sensor and recording package developed by grant NSG-5072 consists of a rotational transducer that converts displacement to voltage. With minor modifications to the sea-level package we have installed instruments horizontally across twenty open fissures near the Krafla caldera in northern Iceland. The instruments consist of long invar wires held in tension by springs. The wire is passed once round the rotational transducer and gives a displacement sensitivity of 0.1 mm.

We have monitored several inflation/subsidence episodes of the Krafla volcano, although only one of the rifting episodes has migrated south toward our extensometer network. The AGU abstract below summarizes some of the conclusions derived from the investigation. The following pages summarize a few of the important problems we hope to solve from continued operation of the instruments.

GROWTH OF LARGE SCALE GROUND FISSURES DURING RIFTING OF THE PLATE BOUNDARY IN NORTHERN ICELAND

Egill Hauksson (Lamont-Doherty Geol. Obs. and Dept. Geol. Sci. of Columbia Univ., Palisades, New York 10964)
Axel Björnsson (National Energy Authority, Reykjavik, Iceland)
John Beavan and Roger Bilham (both at: Lamont-Doherty Geol. Obs., Columbia Univ., Palisades, NY 10964)

Manual measurements and continuous recordings of displacements across fissures during rifting of the plate boundary in N. Iceland reveal continuous growth of fissures in the Krafla caldera, episodic growth of fissures in the associated N/S trending rift zone, and a contemporaneous closure of fissures adjacent to the rift zone.

The Krafla caldera contains several fissures that open during periods of uplift lasting 4-6 months and that close incompletely in subsidence episodes lasting several hours to a few days. In the four cycles we have observed since 1977, we find that maximum rates of opening occur halfway through the uplift period at approximately 1 mm/day. Closing at rates of approximately 10 mm/day starts 3 to 7 hours after volcanic tremors signal the onset of subsidence.

During the September 1977 subsidence, fissure growth migrated southward in three distinct phases: first a slow one-hour aseismic opening phase propagating with a speed of 0.8 m/s from the caldera 12 km along the rift; secondly, a five-hour opening phase propagating south at 0.5 m/s associated with seismicity and magma migration; and thirdly an aseismic recovery phase in which the fissures closed about 25% of the maximum opening at an exponentially decreasing rate with a time constant of approximately 1 day.

Stress Measurements and Rifting in Iceland

Iceland's unique position on the mid-Atlantic ridge commonly evokes an assumption that the lithosphere beneath Iceland is in a state of tension normal to the ridge. For example, a recent spreading episode in northern Iceland can be readily explained in terms of an axial rift system that splits episodically during times of high magmatic pressures and in so doing relieves the cumulative tensional strain that has developed from ridge spreading since the previous eruptive phase (Bjornsson et al., 1978). However, there are two fundamental problems to such an interpretation. Firstly, measurements of absolute stress in several parts of Iceland indicate that the crust is in compression (Hast, 1973; Haimson, 1978, 1979). Moreover the maximum compression axis is normal to the axial rift zones; if this compressive stress is general and not purely an artifact of the surface, but extends throughout the crust, an elastic rebound mechanism alone cannot explain the recent rifting episode. Secondly, broad-anticlinal folding indicates that compression normal to the ridge axis is a widespread geological phenomenon (Einarsson, 1968).

There are a number of possible explanations for the existence of compressive stresses in Iceland surface materials. Haimson (1978) discusses possible mechanisms and proffers a glacial rebound model with accretion and magma injection occurring during loading. A differential cooling model can also produce surface compression; in this, the surface layers cool first and result in surface tensions. As subsurface layers cool, tensional characteristics are "healed" and the surface layers are eventually compressed. In such a model one might predict compressive stresses to be a function of distance from the axial rift zone and also a function of depth. Other hypotheses are that surface compressional stress can arise from broad synclinal flexures away from the ridge or gravitational loading on an inclined lithosphere.

A suggested mechanism to account for simultaneous rifting and horizontal compression is that magma injection forcibly thrusts the plate boundary apart. A simple model is presented by Koide and Bhattacharji (1976). In this model an oblate ellipsoidal magma chamber exerts lateral compression on adjacent crust but puts the shallow crust above the chamber in tension. This model also results in a reduction of stress with proximity to the axial rift zone.

A weakness of these models is the poor constraints imposed by available data. Stress measurements are few and show values of between 70 and 100 bars at distances of between 60 km and 300 km from rift zones. An important source of information is the recent rifting episode that is occurring in N. Iceland. Bjornsson et al. describe the current rifting episode as a series of cyclic processes involving:

1) Slow inflation (3-6 months) of the Krafla caldera by magma migration into a spherical reservoir at a depth of 3 km (Tryggrasson, 1978).

2) Rapid subsidence of the caldera sometimes but not always accompanied by an eruption.

3) Onset of low stress seismicity and migration of magma south or north into fissures.

4) Sequential and permanent opening of axial fissures and simultaneous closure of fissures outside the rifting region during dyke injection.

5) Elevation of flanks of rift zone relative to central region.

6) Cessation of seismic activity in a few high-stress type earthquakes and end of dyke injection.

It is generally considered that the inflation/deflation episodes of the Krafla caldera involve different processes from the dyke injection episodes that immediately follow deflation. Thus, although it is tempting to interpret the seismic activity signalling the onset of dyke injection as signifying generalized low stress, on account of low b-value measurements (Einarsson, 1978) it must be remembered that the area involved is on either side of the inflated caldera. The inflated caldera imposes relative compression (Koide and Bhattacharji, 1975) on the surrounding materials which it presumably "hydrofractures" when some critical stress is reached. The hydrofracture direction is normal to the direction of maximum compression, which agrees perfectly with direct and indirect measurements of stress in Iceland. Hence it is possibl that large compressive stresses surround the caldera during inflation even thoug low stress drop earthquakes accompany lateral dyke injection.

We discuss the possibility that the cyclic magma injection process can itself provide a source of the observed compressive stress. Observed magmatic pressures appear to be quite low since eruptions do not fountain more than 20-50 m, implying excess surface pressures of the order of 2-6 bars. It is possible to argue that excess pressures at depth are likely to be less since the density of the erupting lava is lower than that of the frozen outgassed host rock. However, in their model, Koide and Bhattacharji assume excess magma pressures of 1000 bars at depths of 10-30 km (Roberts, 1970). The effects of viscous flow as magma tunnels to the surface will result in a significant drop in pressure that is difficult to estimate since we know little concerning the viscosity of the magma at depth and the dimensions of the supply routes. It may be misleading to assume that magma pressures are simply related to eruptive pressures for another reason. Deflation of Krafla is invariably preceded by the onset of dyke injection. We know that the limited magma supply rate filters rapid pressure fluctuations arising at depth. Hence, at the onset of deflation and therefore a few hours before eruption, the magmatic pressure has started to decrease due to the rapid extension of the magma chamber. Our extensometer measurements indicate that the deflation of Krafla is approximately three orders of magnitude faster than the inflation rate (-1 mm/hour against + 2 mm/day). The onset of dyke injection leads to an immediate and much larger decrease in available pressure at the surface. In the model of Bjornsson et al. (1979) the magma in the Krafla caldera redistributes itself into dykes at depths between 3 and 5 km and from seismic evidence this occurs after deflation has commenced (Brandsdottir and Einarsson, 1978).

An interesting geometric condition can arise in the caldera if complete subsidence of the inflated region has not occurred before surface eruption or near-surface dyke injection has commenced (Figure 1). The injected dyke will freeze in contact with the host rock and create a space problem, preventing complete closure in the deflation phase. This will tend to maintain the inflated geometry of the caldera but with an important difference. During inflation the caldera dome was supported from below by magma pressure. During deflation the magma pressure has diminished rapidly and the dome is supported by lateral stresses in the adjacent rock. If the doming is small the gravitationally induced lateral stress can be many orders of magnitude larger than stresses attributable to magma pressure. Indeed, the forces can be so large that if this process is widespread it is difficult to deny that it plays an important role in the generation of horizontal compressive stresses at the ridge axis.

Clearly, the mechanism of dyke injection would be aided considerably by collapse of the caldera dome and lateral wedging. Unfortunately, tilt measurements do not indicate that significant doming occurs anywhere except near the caldera so that it is unjustifiable to assume the process generally occurs along the rifting boundary. The wedging mechanism may be a purely local effect restricted to the Krafla caldera. Nevertheless it is interesting to speculate whether a similar mechanism might not on a scale of several hundred kilometers be responsible for ridge spreading. The tilts generated by large-scale doming could be sufficiently small to be undetected by levelling or tilt measurements in Iceland yet the result of a rifting episode involving a meter of dyke injection during a meter of uplift and collapse would be to generate horizontal stresses of several kilobars. The stress would appear towards the end of the spreading episode when magmatic pressure diminished and rift activity became dormant. The resulting stresses should give rise to earthquakes on transform faults and the plates within a few active-rifting dimensions from the ridge axis. Transform earthquakes observed a year after spreading support the hypothesis but are insufficient to constrain the model. If sea-level measurements along the Northern Iceland coastline in the next few decades show evidence of widespread deflation or strain and geodetic measurements show an increase in compressive strain normal to the ridge there would be compelling arguments favoring axial wedging as an important aspect of sea-floor spreading. Conversely, if geodetic measurements in future years reveal extension adjacent to the present rifting zone, the mechanism that generates the observed compressive stress is not generated by axial wedging.

The measurements we have initiated will help us understand the mechanism of dyke injection better (Figure 2). The proposed models depend critically on the precise timing of deflation, seismicity, tilt and displacement. The present network of instruments has enabled verification of the dyke injection velocity (5 km/s) estimated from seismic migration by Brandsdottir and Einarsson (1978), and has demonstrated that strain measurements can be used to monitor the subsurface movements of magma in three dimensions. We plan to seek support elsewhere to continue and to expand the measurements to include strainmeters and tiltmeters.

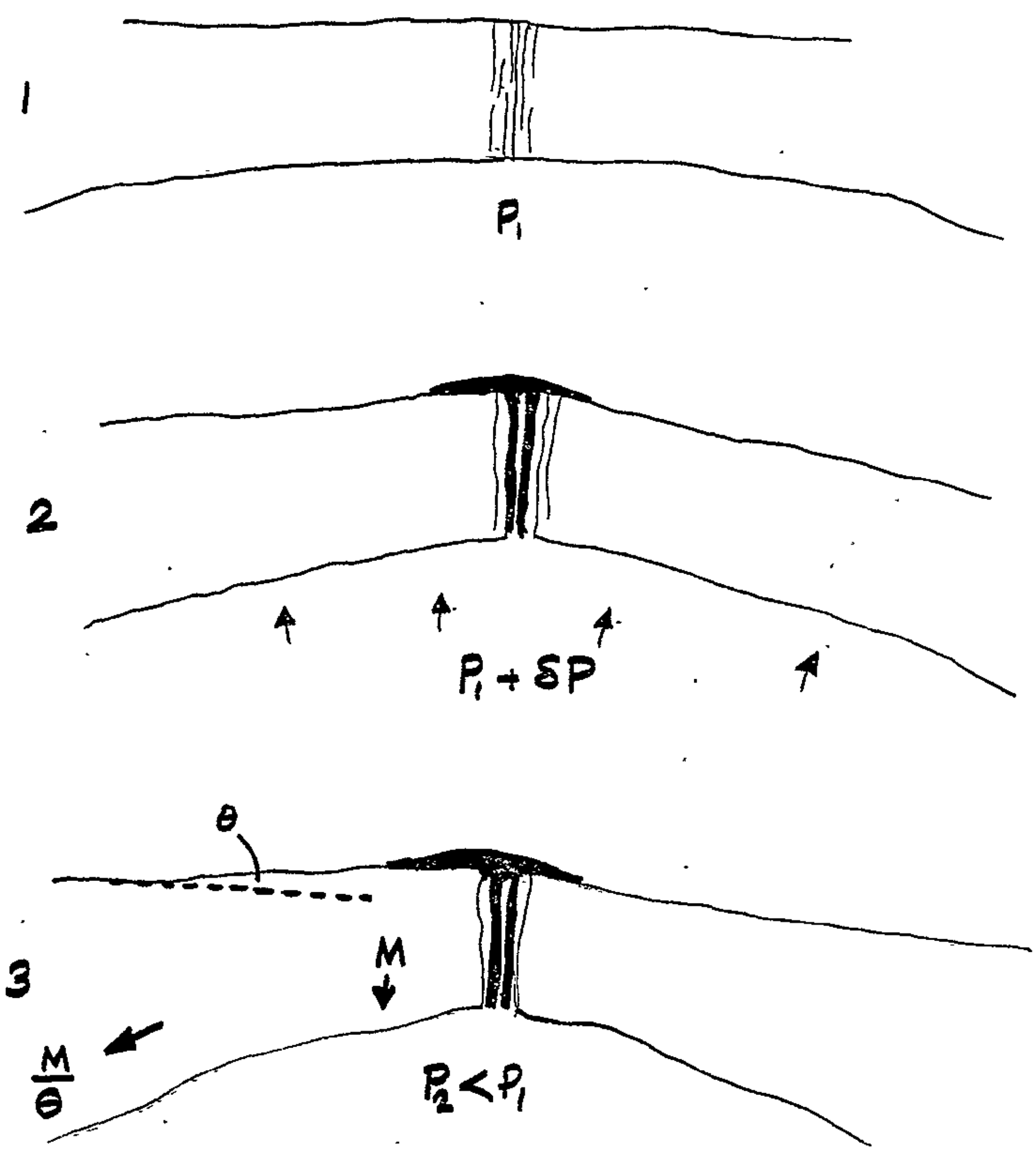

Figure 1. Wedging (3) following injection and freezing of magma (2) on dyke walls resulting from inflation and deflation at ridge axis. The horizontal stresses resulting from cycles of inflation and deflation are proportional to the width of the freshly injected dyke, to the uplift at the time of freezing and to the final magma pressure P_2. If the domal tilt is small ($< 10^{-3}$ radians and $P_2 << P_1$ the force will be $M\theta^{-1}$ where M is the weight of the unsupported dome.

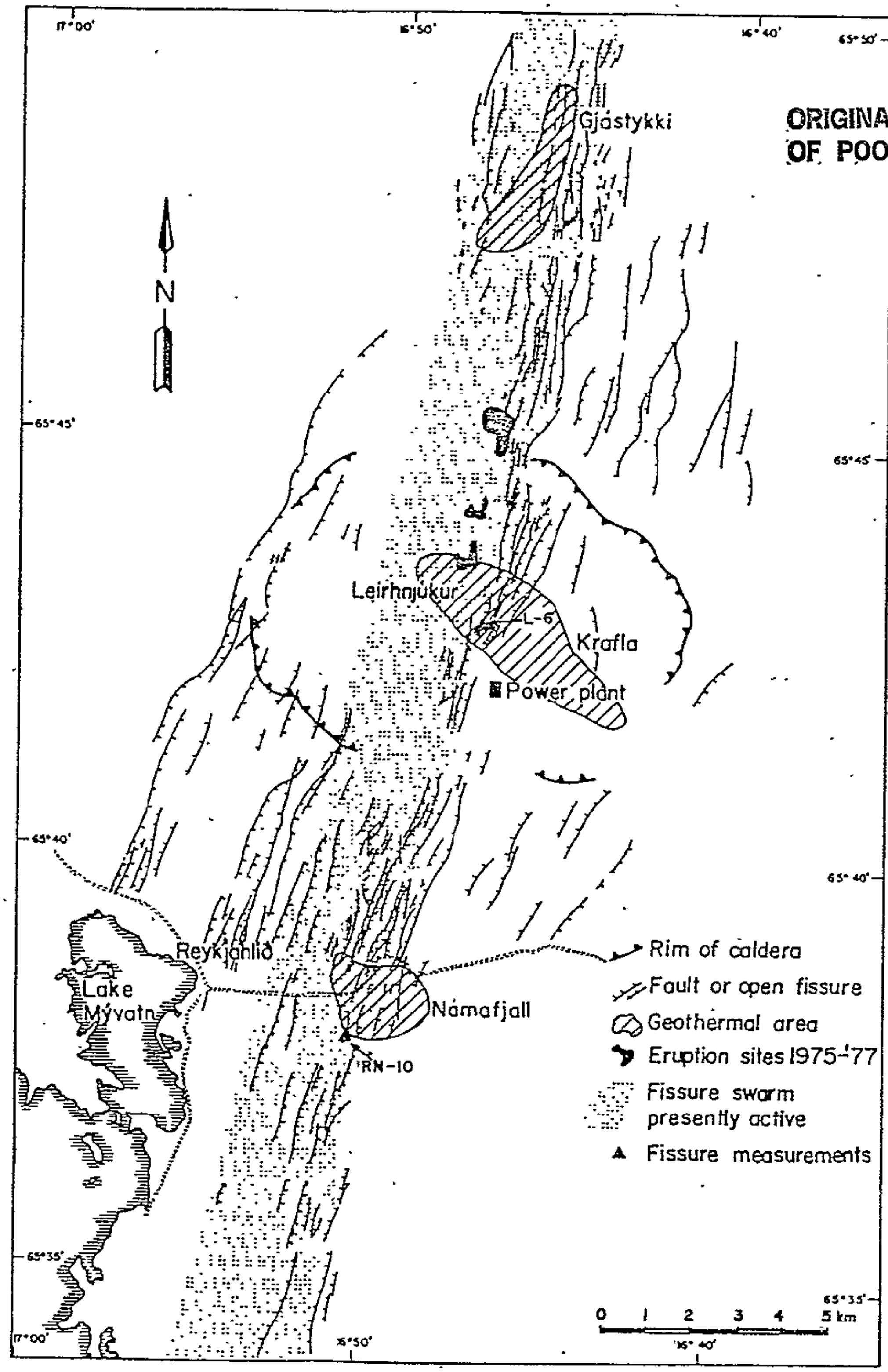

Figure 2. Outline geological map of the Krafla caldera and the associated fissure swarm (from Bjornsson et al., 1976).

References

Björnsson, A., G. Johnsen, S. Sigurdsson, G. Thorbergsson, and E. Tryggrason, 1978, Rifting of the plate boundary in N. Iceland 1975-1978, National Energy Authority OS-JHD-78-21.

Brandsdottir, B., and P. Einarsson, 1978, Seismic activity associated with the September 1977 deflation of the Krafla central volcano in N. E. Iceland, Science Institute, University of Iceland RH-78-13, Reykjavik.

Einarsson, P., 1978, S-wave shadows in the Krafla caldera in N. E. Iceland, Evidence for a magma chamber in the crust, Science Institute, University of Iceland RH-78-9, Raykjavik.

Haimson, B. C., 1979, New stress measurements in Iceland reinforce previous hydrofracturing results: σ_H max is perpendicular to the axial rift zones, EOS (Abstract), AGU Spring Meeting 1979, Washington, D.C.

Haimson, B. C., and B. Voight, 1977, Crustal stress in Iceland, Pure Appl. Geophys., 115.

Koide, H., and S. Bhattacharji, 1975, Mechanistic interpretation of rift valley formation, Science, 189, 791-793.

Roberts, J. L., in Mechanism of Igneous Intrusion, edited by G. Newalt and N. Rast, p. 187, Gallery, Liverpool, 1970.

Tryggrason, E., 1978, Tilt observations in the Krafla-Myvatn area 1976-1977, Nordic Volcanological Institute, 78.02, University of Iceland, pp. 45.

Section 4

Tilts and Strains on Crustal Blocks

Following a study of precise levelling data from Japan we believe that slow movements of crustal blocks with dimensions between several km and several 100 km occur in regions of intense deformation. We argue that such behavior will confuse the interpretation of strain, tilt and vertical deformation data if investigators are unaware of its existence near instrumental locations. We examine the probable elastic and visco-elastic effects of surface block fragmentation and provide a number of examples of strain data that support the existence of active blocks. A fundamental difficulty in identifying block fragmentation exists if levelling data are not available. In such circumstances (e.g., island arcs) it is vital to monitor tilt and vertical movements (sea-level measurements) to fully understand tectonic deformation.

STRAINS AND TILTS ON CRUSTAL BLOCKS

R.G. BILHAM AND R.J. BEAVAN

Lamont-Doherty Geological Observatory of Columbia University, Palisades, NY 1096

ABSTRACT

Bilham, R.G., and Beavan, R.J., 1977. Strains and tilts on crustal blocks. Tectonophysics,

We present some of the evidence for continental crustal block structures revealed by geodetic work during the last century. Block dimensions ranging from 5 to 50 km appear to be common in regions of intense tectonic activity. The properties of block structures are discussed in terms of the measurement of tectonic deformation by surface strainmeters and tiltmeters. Block boundaries are often significantly weaker than the contiguous crustal blocks they divide and this feature results in the concentration of strains at boundaries and the diminution of strains within blocks. Tilts on crustal blocks can vary in phase and magnitude from block to block. In addition, there is some indication that block boundaries may respond visco-elastically or exhibit strain dependent elastic properties. Such behavior can account for the slow transmission of tectonic deformation reported in Japan and elsewhere. If non-linear behavior is a characteristic of regions fragmented by crustal blocks it introduces problems for the interpretation of observed surface strain and tilt. In particular, it will generally not be possible to apply a site correction factor based on the observed distortion of seismic or tidal strains to the interpretation of secular strains.

Lamont-Doherty Geological Observatory Contribution No. 0000

INTRODUCTION

In recent years the problems of measuring strains and tilts near the Earth's surface have received the attention of numerous authors. Two principal difficulties have been identified as posing serious threats to the effectiveness of surface deformation measurement. The first of these is the distortion of applied strainfields by local elastic inhomogeneity and the second is the existence of noise generated at the Earth's surface by non-tectonic effects. It is now established that strainfield distortion arising from geometric and elastic inhomogeneity can be estimated with reasonable precision (Berger and Beaumont, 1976; King et al., 1976), and some progress has been made in discriminating between certain types of surface noise and signals of tectonic interest (Wood and King, 1977). New instruments with longer baselines may also result in improved data (Davis et al., 1978).

We are concerned about a more fundamental problem associated with measuring strains and tilts near the surface. There is considerable evidence that parts of the Earth's crust behave as a mosaic of loosely-coupled blocks. Ca surface fragmentation result in behavior that cannot be predicted in terms of linear elastic theory? Non-linear behavior may result in the failure of several assumptions. For example, if block interaction is frequency dependent, it is clearly incorrect to assume that the response of a region to periodic tidal strains is the same as the response of the region to secular strains. If the coupling of blocks is stress dependent, the transmission of strains and tilts across a region may exhibit phase and magnitude anomalies not predicted by present inhomogeneity theory. It is clearly of the utmost importance to clarify the influence that block structures may have on surface strainfields and tiltfields.

GEODETIC EVIDENCE FOR CRUSTAL BLOCKS

Although geodetic survey data of high quality have been obtained in many parts of the world in the last century, it is only in Japan that large numbers of strainmeters and tiltmeters have been operated simultaneously for many years (Harada, 1976; Hosoyama, 1976). The results of geodetic relevelling rather than trilateration or triangulation are of interest since the precision obtained by levelling is systematically better than other techniques at any given time and also because the distribution of fixed benchmarks (approximately 2 km spacing in Japan) is far denser than triangulation or trilateration points.

In the late 1920's and early 1930's, a series of papers describing relevelling lines in Japan were published by some half-dozen authors. Pivotal to their interpretation of these levelling data was an intense discussion of block movements which were clearly identified in central and southern Japan (Yamasaki, 1928; Muto and Atsumi, 1929; Imamura, 1930a; Miyabe, 1933; Tsuboi, 1933). The geodetic blocks that were identified were sometimes, but not always, the structural units into which geologists and geomorphologists had subdivided the crust. The Japanese geodetic data present compelling evidence that at least some of the geological processes that gave rise to observed formations are presently active.

In Figures 1-4 we present typical data from the papers of Imamura and Tsubo: that illustrate evidence for block movements. Note that the data presented have not been corrected for "spurious" data points nor have they been smoothed by linear or weighted averaging processes. In many cases the data have not been adjusted for the misclosure of long geodetic lines. The intentional display of raw data enables the identification of discontinuities in the levelling lines if they exist. This is especially easy if several relevelling profiles are available. Unfortunately, spurious benchmark movements can sometimes appear as systematic discontinuities in the data; however, two remaining tests are available. First, the location of the apparent discontinuity can be related to the known geology. In many cases discontinuities correspond to known active faults but occasionally they correspond to "dormant" geological faults (Imamura, 1929 - 1935). Secondly, the discontinuity may coincide with an inflection of the levelling profile that frequent relevelling reveals as a consistent hinge-line about which the adjacent surfaces appear to rotate.

Imamura (1933a) generalized the observed behavior of a sequence of block surfaces into two categories. Surfaces with "N-shaped faults" in which adjacent block surfaces rotate in the same sense and surfaces with "V-shaped faults" where adjacent block surfaces rotate in an opposing sense (Fig. 5). He remarks further that surfaces with multiple N-shaped faults are associated with compressive horizontal strains and that surfaces with V-shaped faults are generally associated with tension. We adhere to Imamura's original visually-descriptive terminology in which he describes the crustal surface pattern in terms of the discontinuities as it has the advantage of brevity. An important property of V-shaped faults is that the hinge-type motion which occurs need not necessarily involve vertical or horizontal offset and therefore the fault may be dismissed as inactive during surface geological mapping. Moreover, if a V-shaped fault is covered by superficial deposits, its presence may only be detectable by geodetic methods (Imamura, 1931). Activity suggestive of V-shaped fault behavior has been reported in California by Buchanan-Banks et al. (1975), Savage et al. (1975), Bennet et al. (1977) and Hill et al. (1977).

Block activity is most pronounced at times of seismic energy release or volcanic activity. Coseismic block motion forms the bulk of the observed phenomena but postseismic activity on boundaries has been documented on numerous occasions (Scholz, 1972). For example, earthquakes in 1925 (Tazima) and 1927 (Tango) activated the same block boundaries (Tsuboi, 1933) but in succeeding years, block motions continued (Figure 1). Imamura (1929) pointed out that block motions associated with the 1923 South Kanto earthquake were bounded by existing geological faults. In the same region, Scholz and Kato (1977) using a seventy year data base with 23 repeat levellings along several levelling lines, showed conclusively that these block boundaries were active in the following 15 year postseismic episode and their presence could still be detected in 1963. Of great significance is their observation that the faults bounding blocks between Tokyo and Atami assume different roles during the various phases of deformation. Thus the Oiso hill block mimics the crustal deformation to the NE between 1924 and 1939 and is decoupled from the SW region by the proposed Odawara fault (Sakawa fault, Imamura, 1930a), whereas between 1939 and 1963 inflection occurs at the Isehara fault such that the Oiso Hill block now follows the general deformation of the region to the SW. In a less conspicuous fashion the faults bounding the Kanagara, Haneda and Omori blocks to the west of Suruga Bay are alternately active and passive between 1883 and 1930 (Imamura, 1931 and Figure 2). Miyabe (1933) notes several examples of adjoining blocks which sometimes move independently and sometimes behave as though locked together.

BLOCK DIMENSIONS

It is of interest to review what is known of the lateral dimensions of observed crustal blocks. Tsuboi (1933) classes <u>minor</u> land blocks as generally being of the order of 7-10 km wide and major blocks approximately 50 km in extent. In the works of Tsuboi and others, smaller and larger blocks are documented. It is significant, however, that the normal 2 km spacing of the Japanese levelling network provides little positive information on the existence of blocks with a width of less than 6 km. The exception to this occurs when a levelling line runs obliquely across an elongated block leading to the detection of block motion but to the overestimation of the block size.

The West-Momaya 4.5 km block was clearly defined by Imamura (1934) using a 500 m spacing of benchmarks near Osaka. Miyabe (1933) argues that secondary block fragmentation down to 1 km may occur based partly on the observation that horizontal strains exceeding 10^{-4} have been measured within 10 km wide blocks. In the Tien Shan region blocks with dimensions of 3-5 km have been documented (Pevnev et. al., 1975) and in Iceland block dimensions of less than 500 m have been reported by Tryggvason (1970, 1974) and Tomasson (1976).

It is curious that the inferred block structures invoked to explain anomalous tilts at tidal periods (Tomaschek and Groten, 1961; Melchior, 1967; Lambert, 1970) and also to explain anomalous tilting in response to atmospheric loading (Tomaschek, 1953, 1959) often require blocks with dimensions exceeding several hundred kilometers. Block dimensions of this size are seldom apparent on geodetic relevelling profiles although oscillatory movements with long wavelengths frequently occur (e.g., Mizoue, 1967). Unfortunately, the tilt data upon which the above-mentioned claims for block structures were based contain systematic errors that were unsuspected by early investigators (King and Bilham, 1973a; Zschau, 1977) and must be regarded as unreliable.

CONSEQUENCES OF BLOCK STRUCTURE

The dangers of measuring surface strain and tilt in the presence of vertical elastic discontinuities have been known for some time (King, 1971; King and Bilham, 1973b). The rigorous correction of tiltmeter data for geometric and elastic inhomogeneities has been achieved recently by Harrison (1976a) and for strainmeter data by Berger and Beaumont (1976) and Levine and Harrison (1976) for a limited number of sites in the USA. The agreement between observed tidal data and predicted values is encouraging (Table 1, italics) and indicates for these sites, as Berger and Beaumont point out, that the elastic theory is complete and that problems of "site" effects can be overcome. In practice this means that a site transfer function can be computed for surface instruments in the presence of gross elastic and topographical inhomogeneities by observing any precisely known strain signal rather than by predicting the effects of the inhomogeneities. King et al. (1976) suggest a method for determining this <u>site tensor</u> which requires the observation of at least three strain signals that must be different but whose amplitudes need not be precisely known.

Can block movements or the presence of crustal blocks result in types of inhomogeneity which cannot be defined in terms of the effects of underground cavities, surface topography and the lateral distribution of elastic moduli? We discuss some of the observed behavior of crustal blocks with this question in mind. In the discussion we frequently make use of the term "applied strain-field". This we define as the strain that would be present on a laterally homogeneous Earth.

(1) Incoherent strainfields. Independent motion of adjacent blocks may give rise to the fragmentation of the applied strainfield into small scale strainfields which are related in a complex way to the applied strainfield. To an observer within the fragmented region, the strains on adjacent blocks could be described as spatially incoherent with each other. However, strains within a block will appear coherent. In the context of the idealized V- and N-shaped faults of Imamura, a strain array between two faults has internal coherence but a strain array with one instrument per block shows poor coherence or no coherence. An important corollary is that if coherent strains or tilts are sought in order to reduce the surface noise in strain or tiltmeter arrays, for example, the spacing of instruments should be much smaller than the block dimensions. Kasahara (1973) argued that the direction and amplitude of tilts and strains measured with tiltmeters and strainmeters at Nokogiriyama and Aburatsubo are not in close agreement with each other or with geodetic data in the same region, and attributed this to inhomogeneity and block structure. Scholz and Kato (1977) demonstrate convincingly that the two observatories are on different crustal blocks which move differently from each other and from the general trend of the region. Yamada (1973) and Shichi (1973), however, reveal a curious similarity between the tilt vectors if the vector coordinates of one station are bilaterally inverted, rotated slightly, an isotropic scaling factor applied and the phase of the Aburatsubo station delayed by about a year. Except for the phase delay, the coordinate transform required can be interpreted as the result of complex block interaction. The phase delay is suggestive of a migrating deformation source (Kasahara, 1977) although it is possible to derive similar delays by invoking non-linear elastic behavior at block boundaries (5 below).

An important feature of surface strainfields is that although topographic and elastic inhomogeneity can distort applied strain amplitudes considerably the rotation of the principal strain axes is minimal (Berger and Beaumont, 1976). It is possible, however, that a mosaic of loosely-coupled blocks might introduce large rotations of the applied strain axes under certain conditions. For example, if a strainfield is applied to one side of a sequence of crustal blocks, the observed strains well into the fragmented region may be largely those arising from random contacts on block boundaries.

(2) Strain attenuation: tilt enhancement. Horizontal strains within a block bounded by free surfaces will tend to zero although the decoupled block will respond to basal tilts. This suggests an argument in favor of using geodetic levelling to search for the existence of active blocks. In practice it is not possible for a fissure to remain open at any great depth (e.g., Reasenberg and Aki, 1974) so that strains will be diminished to a marked degree only near the block boundaries and according to the degree and depth of the weaker boundary zone. Latynina (1975b) reasons that vertical discontinuities may be widespread, resulting in a global attenuation of tidal strain. Recent observations of tidal strain do not favor this hypothesis. In Table I, we compile tidal admittance results from several observatories. The admittance is the ratio of the observed tidal strain amplitude to the combined amplitude of the theoretical tide and the estimated ocean-loading strain tide. Figures in italics are the tidal admittance after correction for the distorting effects of local cavities, surface topography and known geology. Unity admittance and zero phase are expected where the predicted value agrees with the observations. Although the average tidal admittance is low for data

where site corrections have not been applied, it would appear that except in a few cases, site geometry can account for much of the observed attenuation (Berger and Beaumont, 1976). The lack of evidence for a general attenuation of strain amplitudes at tidal frequencies need not necessarily exclude the occurence of crustal blocks if block boundaries behave viscoelastically.

(3) Strain concentration at block boundaries. Strain applied to a region of elastic contrast will concentrate in the relatively compliant zones. That block boundaries are generally zones of low elastic moduli has been substantiated by many investigators. Seismic velocity anomalies associated with major faults have been reported by Alewine and Heaton (1973), Bakun and Bufe (1975), and Healy and Peake (1975). In a finite element model of the San Andreas fault zone, Wood et al. (1973) show that tidal tilts are particularly sensitive to the effective stiffness of the fault zone. The enhancement of strains across a block boundary was studied by Latynina (1975a,b) who reports tidal strain magnifications of 100% across parts of the Kondarinsky fault and abnormally large secular strains. Tidal strains within the San Andreas fault zone are not reported although the apparent modulation of the velocities of seismic waves traversing the zone suggests substantial enhancement (McEvilly and Johnson, 1977). Discrepancies in the magnitudes of transient tilts measured by tiltmeters near the San Andreas fault zone are presumably caused by contrasting rock types (McHugh and Johnston, 1976) although these data were not corrected for topographic effects. The effects of varying the shear modulus in the zone are discussed by McHugh and Johnston (1977).

(4) Local block boundary strains. Differential movement of adjacent blocks may generate local strains at block boundaries. Local strainfields may be generated near locally rigid asperities on adjoining block surfaces.

They are important because they will generally occur at the same times as changes in the applied strains inducing block motion. Consequently, it will be difficult to distinguish between the applied strains and the induced local strainfields, especially if the latter are much larger in magnitude. Whereas strain concentration described in (3) will be restricted to the weak parts of block boundary zones, local strainfields will be transmitted within the adjacent blocks. The principal axes of these induced local strains need not necessarily be the same as the applied primary strains. A possible manifestation of block behavior which may include the generation of local strains is the observation of strain-steps in certain tectonic regions and to the somewhat uneven way which strain-steps have been observed to decay with distance (Jap. Network Crustal Movement Observ., 1970).

The generation of strainfields at block boundaries by non-tectonic stresses may occur. Strain measurements across the Yamasaki fault zone (Oike et al., 1976) indicate that strains within the fault occur at times of heavy rainfall. Similar effects are observed on the Lake Cavazzo fault, Italy (Caloi and Migani, 1972). Tomasson (1976) and Tomasson et al. (1976) present data for a fissured region in Iceland which indicates clearly that block movements are related to water-table changes. Herbst (1976) proposes a model for near-surface, hydraulically-induced tilt noise that requires a similar mechanism.

(5) Non-linear elastic behavior. As has been remarked before, adjoining blocks do not always move independently but sometimes appear to coalesce and behave as a larger unit. Is this to be interpreted as a variation of the properties of a fault zone subject to a uniform applied strain or as the response

of weakly-coupled blocks to changing applied strainfields?

Evidence of short-term elastic moduli changes may be found in the study of the Kondarinsky fault zone, north of Dushambe, Tadjikistan. Figure 6 is compiled from Gzovsky et al. (1972), Latynina et al. (1974), and Latynina and Rizaeva (1976). During the first few months of 1967, strains across part of the fault indicate compression and insignificant tidal amplitude variation. In about July a decrease in the strain rate occurs and at about the same time the fault zone stiffness increases as indicated by the decrease in tidal admittance. The compression of the fault zone resumes when the tidal amplitude assumes its former value. The observed elastic modulus change is transitory and does not coincide closely with the strain compression data. Nonuniform compression of the fault zone is to be expected in view of the probable uneven boundaries between the two blocks and this may account for the lack of closer agreement of the two curves.

Flexing of block boundaries characteristic of V-shaped faults may give rise to time dependent changes in elastic modulus or viscoelastic behavior. For small variations about a quiescent strain level in the fault zone, the block boundary may behave linearly but if the strain departs significantly from this level, the fault zone may exhibit non-linear properties.

It is interesting to combine the properties of a viscoelastic material with the additional constraint of non-linear elasticity within the fault zone. A simple model is shown in Figure 7. For rapid strains over a small range, the elastic properties of k_1 are dominant. For slowly applied compressive strains, the system has negligible stiffness until k_2 is engaged. If the stiffness of k_2 approaches that of the block material, displacements are transmitted across the system with good fidelity at all frequencies. Experimental evidence for fractured rock behaving in this way is presented by Goodman (1976, p. 172). An important feature of the model is that it enables the transmission of long-period (secular) deformation with a delay. A series of such block boundaries could result in an extremely slow (delay-line) propagation of crustal strain. A second feature of the model is the increase in strain rate that accompanies the eventual transmission of the applied strain. These two characteristics of the model agree with the observed tilt data from Japan where slow propagating tilts are recognized by rapid inflections in tilt vectors (Kasahara, 1977). The model allows the propagation of crustal deformation without the entity of a deformation front (Scholz, 1977; Kasahara, 1977) or a strain wave (Bott and Dean, 1973; Spence, 1977); however, it still requires the existence of a remote source of strain to initiate the disturbance. A discussion of the physical conditions resulting in behavior similar to the proposed model is outside the scope of the present article, although it is probable that the role of fluids is significant.

CONCLUSIONS

We have reviewed some of the evidence for block motion in areas of intense tectonic deformation. It is important to understand whether active block structures occur in a given area where strainmeters or tiltmeters are to be installed singly or in arrays, since some of the elastic properties of the resulting surface fragmentation can cause interpretive ambiguity in observed data. In general, observed strainfields will be incoherent across block boundaries compared to strains within integral blocks. Strain magnitudes can be reduced significantly within blocks which may exhibit large tilts. The azimuth of observed principal strain axes may differ from the azimuth of applied strain axes in places where local strainfields are generated at block boundaries. Applied strains will normally be intensified at block boundaries if these are represented by relatively weak fault zones.

In many ways the effects of crustal blocks can be described in terms of geometrical and geological inhomogeneities (Harrison, 1976b; Blair, 1977). The theory developed for treating these forms of inhomogeneity assumes linear elasticity. It is possible, however, that some block boundaries must be modelled as non-linear rheological systems involving frequency dependent or strain-dependent elastic properties. If these occur, their effects do not appear to modify tidal strains significantly (Levine and Harrison, 1976; Beavan and Goulty, 1977), although they may affect secular strains. A possible strain-delay mechanism based on viscoelastic, block-boundary behavior is suggested that can account for the slow transmission of secular tectonic signals.

Blocks with surface dimensions ranging from below 1 km to greater than 50 km have been inferred. Though not of great tectonic significance, blocks with dimensions of a few kilometers potentially create serious difficulties to the interpretation of strainmeter or tiltmeter data. A history of levelling data can reveal the presence of active block motion in a given region better than other geodetic techniques since the density of fixed markers is greater than for triangulation or trilateration data, the precision is consistently good and, in Japan at least, the identification of active block motion is assisted by the recognition of discontinuous surface tilt. For this application, it is permissible to use parallel nearby relevelling profiles which may not have a common datum. Normal geodetic levelling data, however, will not reveal blocks with dimensions less than about 5 km. The density of strainmeters or tiltmeters required in regions in which blocks may be less than a few kilometers is clearly economically prohibitive. A compromise between a dense array of continuously monitoring instruments and frequently repeated geodetic work is indicated in which the spacing of fixed reference markers is some fraction of a kilometer.

An understanding of the behavior of crustal blocks and block boundaries is important if we are to interpret long-period strainmeter and tiltmeter data. The study of block boundaries is a promising area for future research.

ACKNOWLEDGEMENTS

We are indebted to Chris Scholz who drew our attention to the wealth of geodetic data published by Japanese researchers and who has provided considerable encouragement for the work. Klaus Jacob and Lynn Sykes have read the manuscript critically and suggested several improvements.

The work has been supported by NSF (EAR 76 03957) and NASA.

REFERENCES

Alewine, R.W. and Heaton, T.H., 1973. Tilts associated with the Pt. Mugu earthquake. Proc. Conf. Tectonic Prob. San Andreas Fault System, Stanford University, XIII: 94-103.

Bakun, W.H. and Bufe, W.H., 1975. Shear wave attenuation along the San Andreas fault zone in central California. Bull. Seismol. Soc. Am., 65: 439-459.

Beaumont, C. and Berger, J., 1975. An analysis of tidal strain observations from the United States of America: I. The homogeneous tide. Bull. Seismol. Soc. Am., 65: 1613-1629.

Beavan, R.J., 1976. Earth strain: ocean loading and analysis. Ph.D. Thesis, Cambridge University.

Beavan, R.J. and Goulty, N.R., 1977. Earth strain observations made with the Cambridge laser strainmeter. Geophys. J. R. astr. Soc., 48: 293-305.

Bennet, J.H., Taylor, G.C., and Toppozada, T.R., 1977. Crustal movement in the Northern Sierra, Nevada. California Geology, 30: 51-60.

Berger, J. and Beaumont, C., 1976. An analysis of tidal strain observations from the United States of America: II. The inhomogeneous tide. Bull. Seismol. Soc. Am., 66: 1821-1845.

Blair, D., 1977. Topographic, geologic and cavity effects on the harmonic content of tidal strain. Geophys. J. R. astr. Soc., 48: 393-405.

Bott, M.H.P. and Dean, D.S., 1973. Stress diffusion from plate boundaries. Nature, 243: 339-341.

Buchanan-Banks, J.M., Castle, R.O., and Ziony, J.I., 1975. Elevation changes in the central transverse ranges near Ventura, California. Tectonophysics, 29: 113-125.

Caloi, P. and Migani, M., 1972. Movements of the fault of the Lake of Cavazzo in connection with local rainfalls. Ann. Geofis., 25: 15-20.

Davis, P., Evans, K., Horsfall, J., and King, G., 1978. Long baseline tilt and strain measurement. Recent Crustal Movement Symposium, this volume.

Evans, J.R., 1975. Spatial inhomogeneity of the Earth strain tide. Ph.D. Thesis, Cambridge University.

Goodman, R.E., 1976. Methods of Geological Engineering in Discontinuous Rocks. West Publ. Co., pp. 472.

Gzovsky, M.V., Latynina, L.A., Ostrovsky, A.E., and Pevnev, A.K., 1972. Slow deformations of the Earth's crust and their relation to earthquake in the U.S.S.R. Phys. Earth Planet. Int., 6: 235-240.

Harada, T., 1976. Accumulation of data by the Geographical Survey Institute. J. Geod. Soc. Jap., 22: 228-234.

Harrison, J.C., 1976a. Tilt observations in the Poorman Mine near Boulder, Colorado, J. Geophys. Res., 81: 329-336.

Harrison, J.C., 1976b. Cavity and topographic effects on tilt and strain measurements. J. Geophys. Res., 81: 319-328.

Healy, J.H., and Peake, L.G., 1975. Seismic velocity structure along a section of the San Andreas fault near Bear Valley, California. Bull. Seismol. Soc. Am., 65: 1177.

Herbst, K., 1976. Interpretation von Neigungsmessungen im Periodenbereich oberhalb der Gezeite. Ph.D. Dissertation: Techiuchen Universitat Calusthal.

Hill, R.L., Sprotte, E.C., Bennet, J.H., and Slade, R.C., 1978. Fault location and fault activity assessment by analysis of historic level line data, oil well data and ground water data, Hollywood area, California, Recent Crustal Movements Symposium, This volume.

Hosoyama, K., 1976. Observational accuracy of crustal movements. J. Geod. Soc. Jap., 22: 235-241.

Imamura, A., 1929. On the multiple source of origin of the Great Kwanto earthquake and its relation to the fault system connected with the earthquake. Proc. Imp. Acad. Jap., 5: 330-333.

Imamura, A., 1930a. Topographical changes accompanying earthquakes or volcanic eruptions. Publ. Earthquake Invest. Comm. in foreign languages, 25: 1-143, Tokyo, Japan.

Imamura, A., 1930b. On the block movement accompanying and following the Great Kwanto earthquake of 1923. Proc. Imp. Acad., Japan, 6: 415-418.

Imamura, A., 1930c. On the chronic block movements in the Kyoto-Osaka district. Jap. J. Astr. Geophys., 7: 93-101.

Imamura, A., 1930d. On changes of topography, both chronic and acute in the southern part of Sikoku. Proc. Imp. Acad. Jap., 7: 101-104.

Imamura, A., 1931. On the northward movement of crustal deformation along the western boundary of the Kwanto plain. Proc. Imp. Acad. Jap., 7: 315-318.

Imamura, A., 1932a. On slow changes of land level, both related and unrelated to earthquakes. Proc. Imp. Acad. Jap., 8: 247-254.

Imamura, A., 1932b. Further studies on the block movement of the Kii, Peninsula. Proc. Imp. Acad. Jap., 8: 163-166.

Imamura, A., 1933a. On crustal deformations preceding earthquakes. Jap. J. Astr. Geophys., 10: 82-92.

Imamura, A., 1933b. On the crustal deformations that preceded and accompanied the severe Haneda earthquake of August 3, 1926. Proc. Imp. Acad. Jap., 7: 271-274.

Imamura, A., 1933c. On crustal deformation in west-central Kii Peninsula. Proc. Imp. Acad. Jap., 9: 39-42.

Imamura, A., 1934. Chronic movements of a minor crustal block as revealed by the revision of a levelling line into one with closely-spaced benchmarks. Proc. Imp. Acad. Jap., 10: 69-72.

Imamura., A., 1935. Crustal deformations associated with the Dewa earthquakes of 1804 and 1894 as revealed through revisions of precise levels. Proc. Imp. Acad. Jap., 11: 51-54.

Japanese Network of Crustal Movement Observatories, 1970. Spatial distribution of strain steps associated with the earthquake of the central part of Gifu Prefecture, Sept. 9, 1969. Bull. Earthq. Res. Inst., 48: 1217-1233.

Kasahara, K., 1973. Earthquake fault studies in Japan. Phil. Trans. R. Soc. Lond., A274: 287-296.

Kasahara, K., 1977. Migration of crustal deformation. Recent Crustal Movements Symposium, this volume.

King, G.C.P., 1971. The siting of strainmeters and tiltmeters for teleseismic and tidal studies. Bull. R. Soc. New Zealand, 9: 239-247.

King, G.C.P. and Bilham, R.G., 1973a. Tidal tilt measurement in Europe. Nature, 243: 74-75.

King, G.C.P. and Bilham, R.G., 1973b. Strain measurement instrumentation and technique. Phil. Trans. R. Soc. Lond, A274:

King, G., Zurn, W., Evans, R. and Emter, D., 1976. Site correction for long-period seismometers, tiltmeters and strainmeters. Geophys. J. R. Astron. Soc., 44: 405-411.

Lambert, A., 1970. The response of the Earth to the ocean tides around Nova Scotia. Geophys. J. R. astr. Soc., 19: 449.

Latynina, L.A., 1975a. On horizontal deformations at faults recorded by extensometers. Tectonophysics, 29: 421-427.

Latynina, L.A., 1975b. On the possibility of studying faults in the Earth's crust on the basis of tidal linear strains. Izv. Earth Physics, 3: 16-26.

Latynina, L.A., Karmaleiva, R.M., Rizaeva, S.D., Starkova, E.Y., and Mordonov, B., 1974. Deformation of the Earth's surface at before the earthquake of 3-x-1967. The Search for Earthquake Forerunners at Prediction Test Fields, Nauka, Moscow (in Russian).

Latynina, L.A. and Rizaeva, S.D., 1976. On tidal strain variations before earthquakes. Tectonophysics, 31: 121-127.

Levine, J., 1977. Strain tide spectroscopy. Geophys. J. R. astr. Soc., in press.

Levine, J. and Harrison, J.C., 1976. Earth tide strain measurements in the Poorman Mine near Boulder, Colorado. J. Geophys. Res., 81: 2543.

McEvilly, T.V. and Johnson, L. R., 1977. In-situ seismic wave velocity monitoring. National Earthquake Hazards Program, USGS Semi-Annual Tech. Rept. Summ., 4: 51.

McHugh, S. and Johnston, M.J.S., 1976. Short-period nonseismic tilt perturbations and their relationship to episodic slip on the San Andreas fault in central California. J. Geophys. Res., 81: 6341.

McHugh, S. and Johnston, M.J.S., 1977. Surface shear stress, and shear displacement for screw dislocations in a vertical slab with shear modulus contrast. Geophys. J. R. Astron. Soc., in press.

Melchior, P.J., 1967. Oceanic tidal loads and regional heterogeneity in western Europe. Geophys. J. R. Astron. Soc., 14: 239-244.

Miyabe, N., 1933. Block movements of the Earth's crust in the Kwanto district. Bull. Earthq. Res., Inst., 11:

Mizoue, M., 1967. Modes of secular movements of the Earth's crust, Part 1. Bull. Earthq. Res. Inst., 45: 1019-1090.

Muto, K. and Atsumi, K., 1929. An investigation into the results of the new and old measurements of the levelling net in the Kwanto district. Bull. Earthq. Res. Inst., 7: 495-522.

Oike, K., Kishimoto, Y., Nakamura, K. and Nakahori, Y., 1976. Some characteristic behaviors of the Yamasaki fault zone observed by extensometers. J. Geod. Soc. Jap., 22: 284-285.

Pevnev, A.K., Guseva, T.V., Odinev, N.N., and Saprykin, G.V., 1975. Regularities of the deformations of the Earth's crust at the joint of the Pamirs and Tien-Shan. Tectonophysics, 29: 429-438.

Reasenberg, P., and Aki, K., 1974. A precise, continuous measurement of seismic velocity measurement for monitoring in situ stress, J. Geophys. Res., 79: 399-406.

Savage, J.C., Church, J.P, and Prescott, W.H., 1975. Geodetic measurement of deformation in Owens Valley, California. Bull. Seismol. Soc. Am., 65: 865-874.

Scholz, C.H., 1972. Crustal movements in tectonic areas. Tectonophysics, 14: 201-207.

Scholz, C.H., 1977. A physical interpretation of the Haicheng earthquake prediction. Nature, 267: 121-124.

Scholz, C.H., and Kato, T., 1977. The behavior of a convergent plate boundary: Crustal deformation in the South Kanto District, Japan. J. Geophys. Res., in press.

Shichi, R., 1973. J. Geod. Soc. Jap., 19: 4.

Spence, W., 1977. The Aleutian arc: tectonic blocks, episodic subduction, strain diffusion and magma generation. J. Geophys. Res., 82: 213-230.

Tomaschek, R., 1953. Nonelastic tilt of the Earth's crust to meteorological pressure distributions. Geofis. pura. appl., 25: 17-25.

Tomaschek, R., 1959. Schwankurgen tektonischer schollen infolge barometrischer belastungsänderungen. Freiberger Forschungshefte, C60: 35-55.

Tomaschek, R. and Groten, R., 1961. The problem of residual ellipses of tilt measurements. Commun. Obs. and Belgique, Sẽrie Géophysique, 58: 78-92.

Tomasson, H., 1976. The opening of tectonic fractures at the Langalda Dam. Comm. Int. Grands Barrages, 12th Congres des Grands Barrages, Mexico.

Tomasson, H., Gunnarson, H. and Ingolfsson, P., 1976. Langulda veita, National Energy Authority of Iceland, Techn. Rept., August, 1976 (OS-ROD-7642).

Tryggvason, E., 1970. Surface deformation and fault displacement associated with an earthquake swarm in Iceland. J. Geophys. Res., 75: 4407-4422.

Tryggvason, E., 1974. Vertical crustal movement in Iceland. in Kristjansson (ed.), Geodynamics of Iceland and the North Atlantic Area, Reidel Pub., pp. 241-262.

Tsuboi, C., 1933. Investigation on the deformation of the Earth's crust by precise geodetic means. Jap. J. Astr. Geophys., 10: 93-248.

Wood, M.D., Allen, R.V. and Allen, S.S., 1973. Methods for prediction and evaluation of tidal tilt data from borehole and observatory sites near active faults. Phil. Trans. R. Soc. Lond., A274: 245-252.

Wood, M.D., and King, N.E., 1977. Relation between earthquakes, weather and soil tilt. Science, 197: 154-156.

Yamada, J., 1973. A water-tube tiltmeter and its application to crustal movement studies. Rept. Earthq. Res. Inst., 10: 1-147 (in Japanese).

Yamasaki, N., 1928. Report on the precise levellings in the meizoseismal area of the Tango earthquake. Proc. Imp. Acad. Jap., 4: 60.

Zschau, J., 1977. Air pressure induced tilt in porous media. Proc. 8th Int. Symp. Earth Tides, Bonn, 1977.

TABLE I

Tidal data obtained by strainmeters. Sources: 1-16, Evans, 1975; Beavan, 1976 and Beavan and Goulty, 1977; 17, Emter and Beavan (personal communication); 18-23, Beaumont and Berger, 1975 and Berger and Beaumont, 1976; 24, Levine and Harrison, 1976, Levine 1977. Only locations with both diurnal and semidiurnal tidal results are included in the averages. Figures in italics refer to data that have been corrected for local elastic inhomogeneity.

	Location and azimuth (clockwise in degrees from North)	Latitude (degrees North)	Longitude (degrees East)	O_1 Admittance	O_1 Phase (degrees)	M_2 Admittance	M_2 Phase (degrees)
1	Burdale, 146	54.05	-0.68	.70	-7	1.0	-1
2	Queensbury, 45 (laser)	53.77	-1.86	.74	+6	.82	+1
	(mean of 9 wire)			.84	+6	.79	+2
3	Denholme, 128 (mean of 2)	53.78	-1.83	.77	+6	.82	0
4	Clayton, 67	53.77	-1.86	.68	+12	.75	+17
5	Woodhead, 60 (mean of 3)	53.50	-1.37			.46	+3
6	Harecastle, 155 (mean of 3)	53.03	-2.25			.80	-5
7	Haddon, 132	53.19	-1.65			.89	-7
8	Alfreton, 143	53.09	-1.35			1.25	-4
9	Nottingham, 157	52.95	-1.17			.75	+5
10	Colwall, 62 (mean of 3)	52.08	-2.33			.53	-10
11	Mythe, 144	52.00	-2.15			.65	-16
12	Whittington, 70	51.89	-2.00			1.02	+5
13	Chipping Norton, 140	51.95	-1.55	.49	-1	.52	+12
14	Gatesby, 162	52.22	-1.23	1.87	-5	1.02	+6
15	Warden, 150	52.69	-0.38			.18	-16
16	Madingley Rise, 2	52.22	0.09			1.56	+31
17	Schiltach, 2	48.33	8.33	.78	-6	.90	+4
	61			.63	-5	.75	+3
	120			.60	+5	.78	+3
18	Camp Elliot, 45	32.88	-117.10	1.02	+2	.95	+13
	site corrected			*1.00*	*+2*	*.97*	*+13*
19	Pinion Flat (areal)	33.59	-116.46	.80	-6	.96	-1
	site corrected			*.98*	*-5*	*1.12*	*-3*
20	Mina (areal)	38.44	-118.15	.72	+5	.70	-6
	site corrected			*.97*	*+5*	*.99*	*-5*
21	Round Mountain (areal)	38.70	-117.08	.88	-1	.74	+4
	site corrected			*1.02*	*0*	*.89*	*+2*
22	Flat River (areal)	37.83	-90.48	.99	-3	1.08	+7
	site corrected			*.99*	*-3*	*1.08*	*+7*
23	Ogdensburg (areal)	41.09	-74.56	1.01	+5	.96	+3
	site corrected			*.99*	*+4*	*.95*	*+4*
24	Poorman mine, 353	40.03	-105.33	.60	-6	.79	-7
	site corrected			*.81*	*-3*	*1.04*	*-9*
	Average of European observations.			.81	+2	.82	+3
	Average of USA observations.			.86	-1	.88	+2
	Average of site corrected USA observations.			.97	0	1.01	+1

FIGURE CAPTIONS

Figure 1. Block movements in the Tango district (Tsuboi, 1933) during the period May 1927 to September 1930 along a levelling route from Ebara to the Sea of Japan. The Gomura and Yamada faults on which significant postseismic movement was observed, are about 15 km to the east of this north/south line.

Figure 2. Block movements west of Suruga Bay (Imamura, 1931). The upper profile shows changes that may have occurred during the 1923 Kwanto earthquake and the lower curve shows changes after the 1926 Haneda earthquake.

Figure 3. Major land blocks revealed between 1927 and 1894 in a north/south line from Nagaoka to Okitu in Suruga Bay (Tsuboi, 1933).

Figure 4. Block movements between 1888 and 1927 in the region between Ootu and Miyake along the coast of Lake Biwa (Tsuboi, 1933).

Figure 5. Imamura defined block boundary faults as V-shaped or N-shaped depending on whether adjacent block surfaces rotated in opposite or similar directions.

Figure 6. Measurements of secular strain and M_2 tidal amplitude across the Kondarinsky fault zone (Latynina et al., 1974 and Gzovsky et al., 1972).

Figure 7. (a) A viscoelastic model for a block boundary. The upper spring (stiffness, k_1) and dashpot result in viscoelastic behavior. The lower spring is of stiffness, k_2 but is engaged only when the adjoining block surfaces approach and close the gap, L. The stiffness of the system increases when this occurs and the viscous contribution to the overall behavior becomes insignificant if $k_2 >> k_1$. The linear spring and gap, L are a simple approximation to a nonlinear spring whose spring constant increases with compression.

(b) Relationship between applied displacement (u_1) of Block 1 and observed displacement (u_2) of Block 2 for the above model. Between $t = 0$ and $t = t_2$ slow movements of Block 1 are not transmitted to Block 2 although rapid movements are (e.g., at time t_1). After $t = t_2$ the stiffness of the block boundary increases and slow displacements are transmitted, such that $\dot{u}_2 \leq \dot{u}_1$. An important feature of the model is the time delay involved in the transmission of secular block movements.

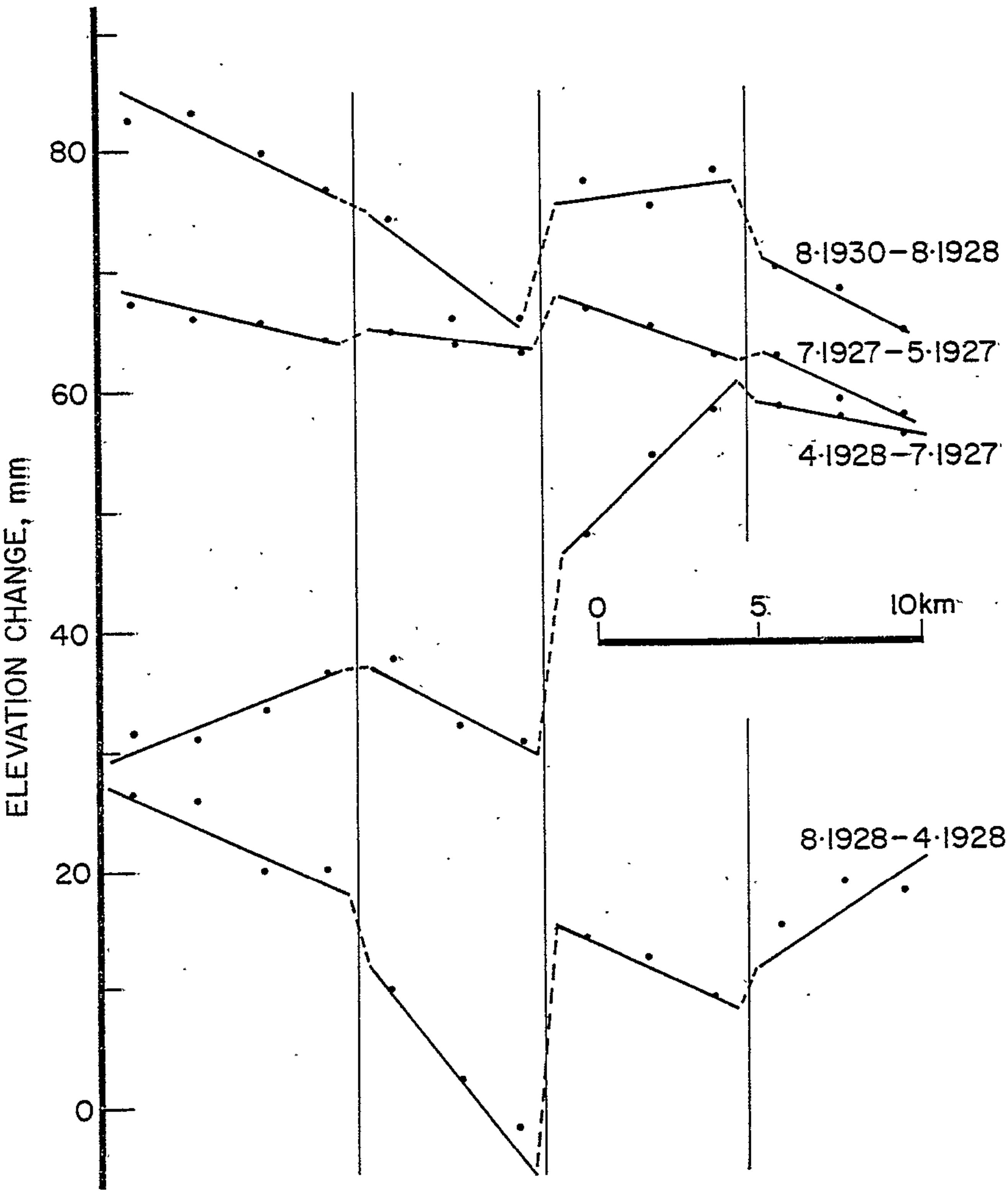
ELEVATION CHANGE, mm
80
60
40
20
0
8·1930–8·1928
7·1927–5·1927
4·1928–7·1927
8·1928–4·1928
0
5
10km

Figure 1

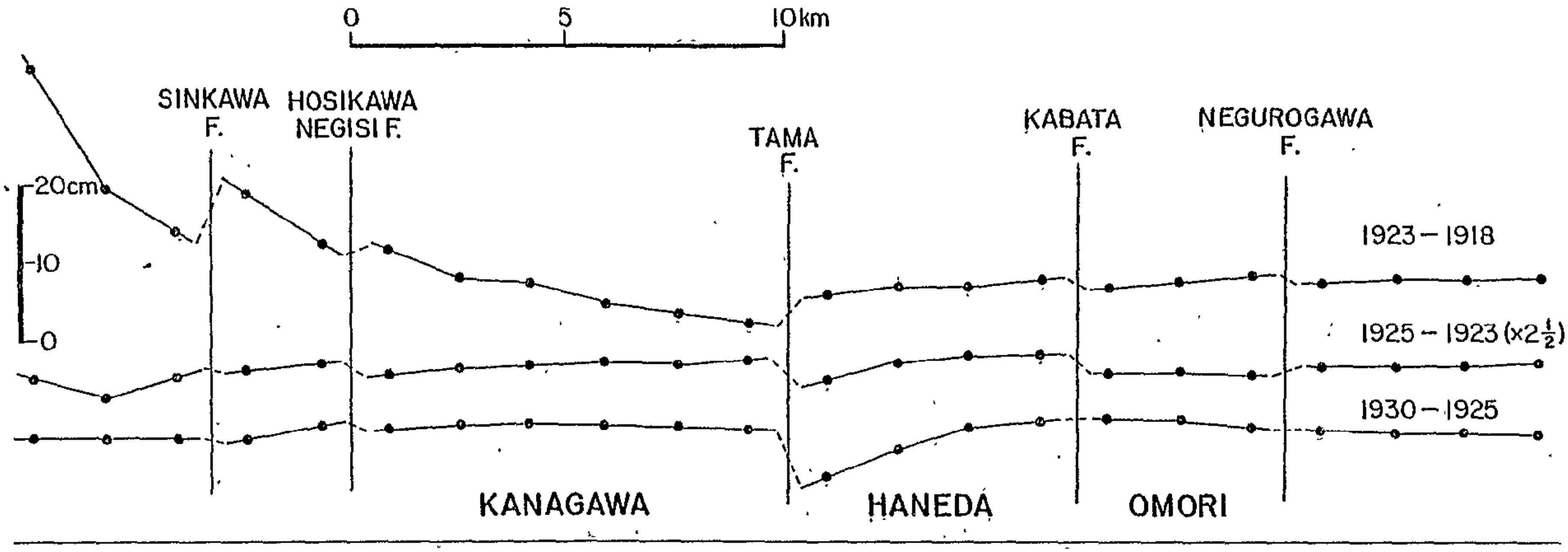
0
5
10km
20cm
10
0
SINKAWA F.
HOSIKAWA NEGISI F.
TAMA F.
KABATA F.
NEGUROGAWA F.
1923 – 1918
1925 – 1923 (×2 1/2)
1930 – 1925
KANAGAWA
HANEDA
OMORI

Figure 2

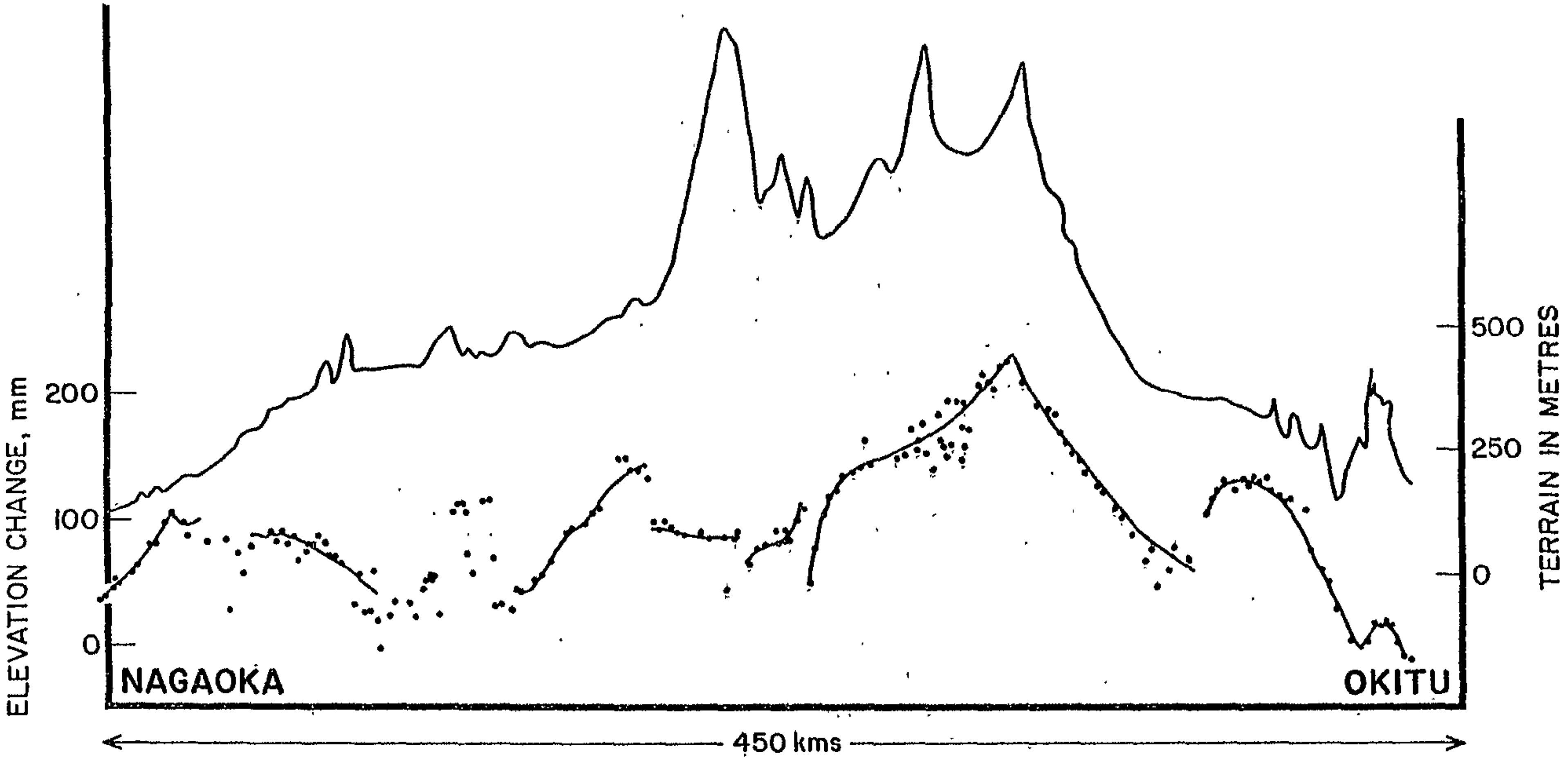
ELEVATION CHANGE, mm
200
100
0
TERRAIN IN METRES
500
250
0
NAGAOKA
OKITU
450 kms

Figure 3

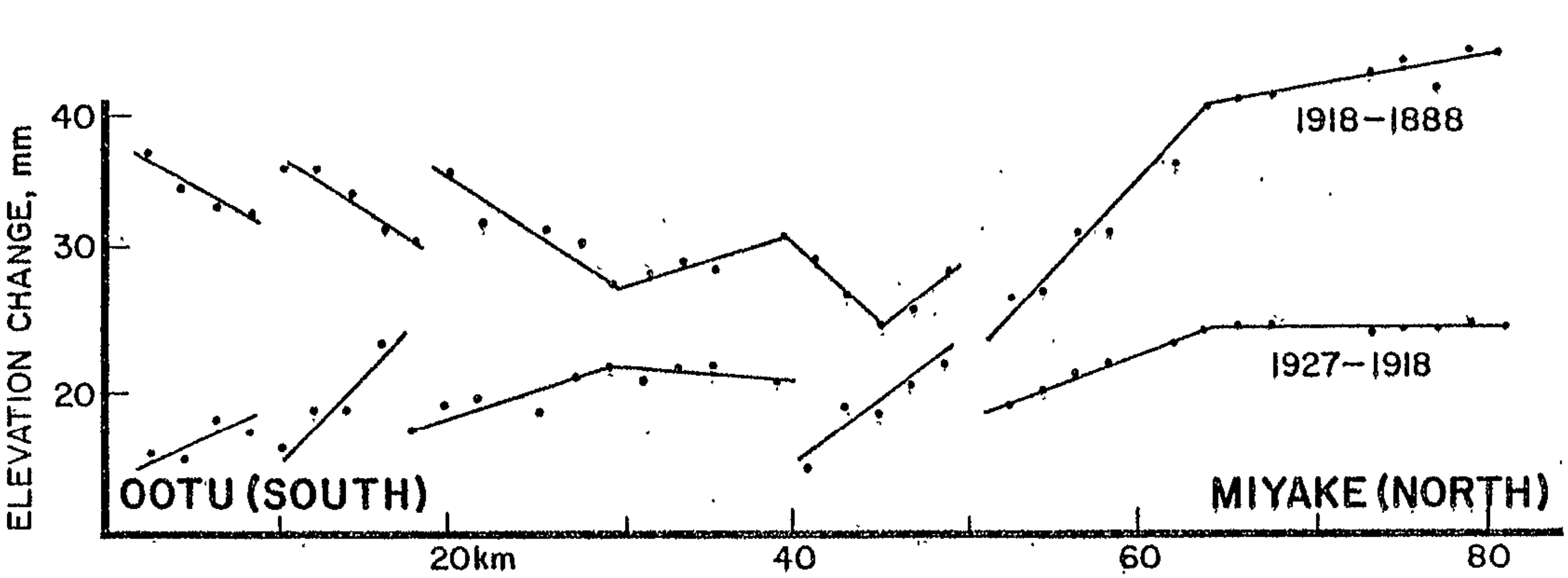
ELEVATION CHANGE, mm
40
30
20
1918–1888
1927–1918
OOTU (SOUTH)
MIYAKE (NORTH)
20km
40
60
80

Figure 4

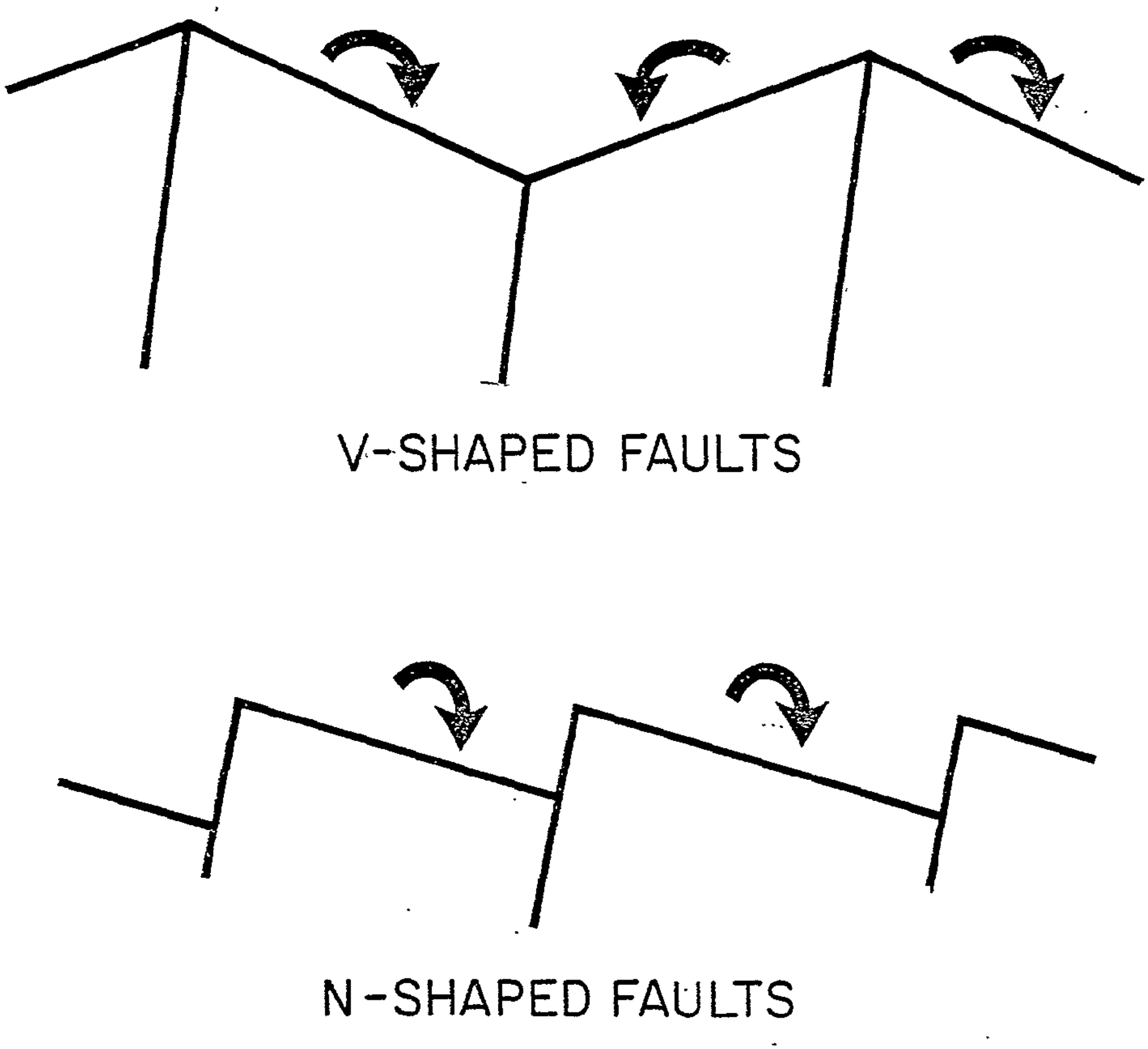

Figure 5

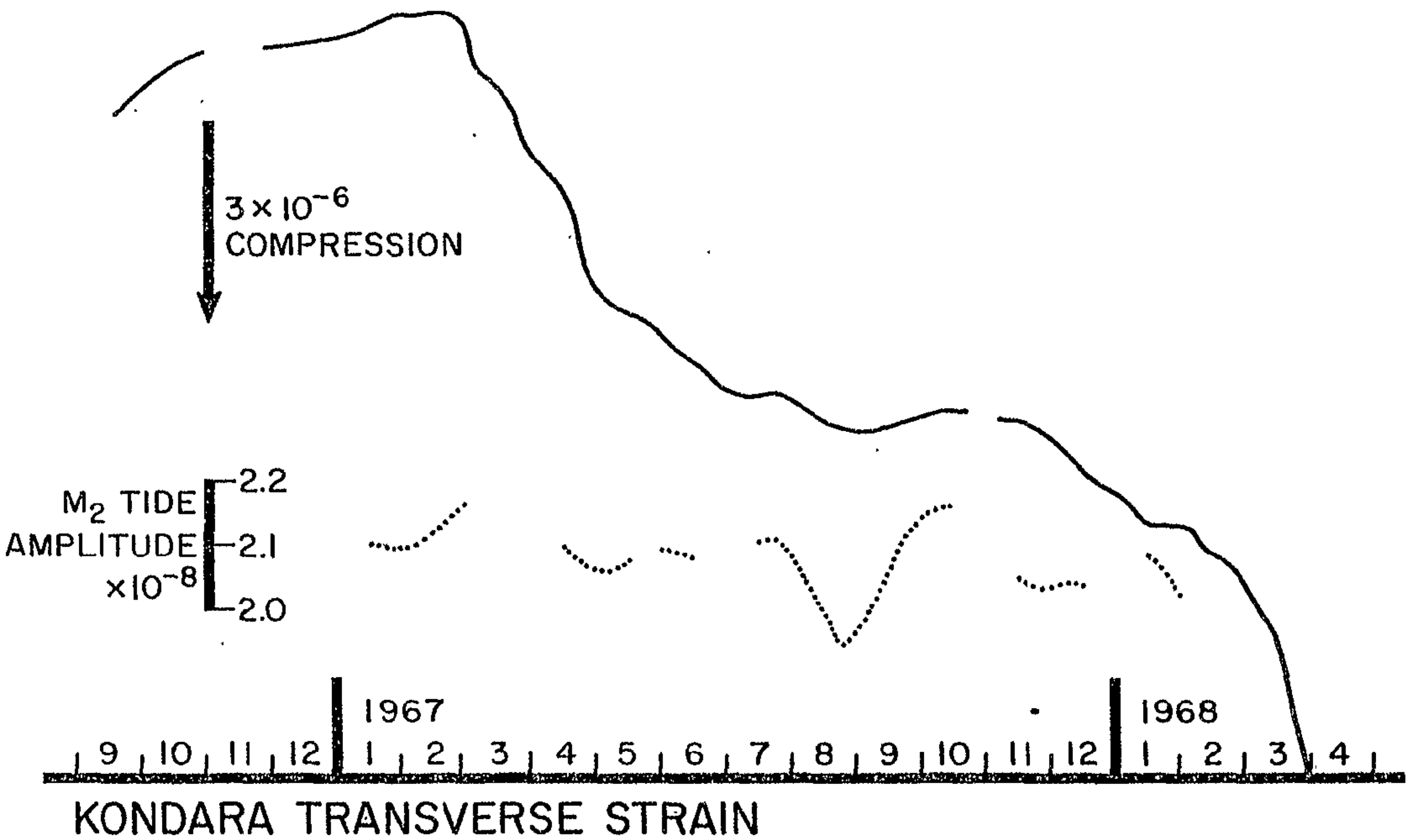
3 × 10⁻⁶
COMPRESSION
M2 TIDE
AMPLITUDE
×10⁻⁸
2.2
2.1
2.0
1967
1968
9 10 11 12 1 2 3 4 5 6 7 8 9 10 11 12 1 2 3 4
KONDARA TRANSVERSE STRAIN

Figure 6

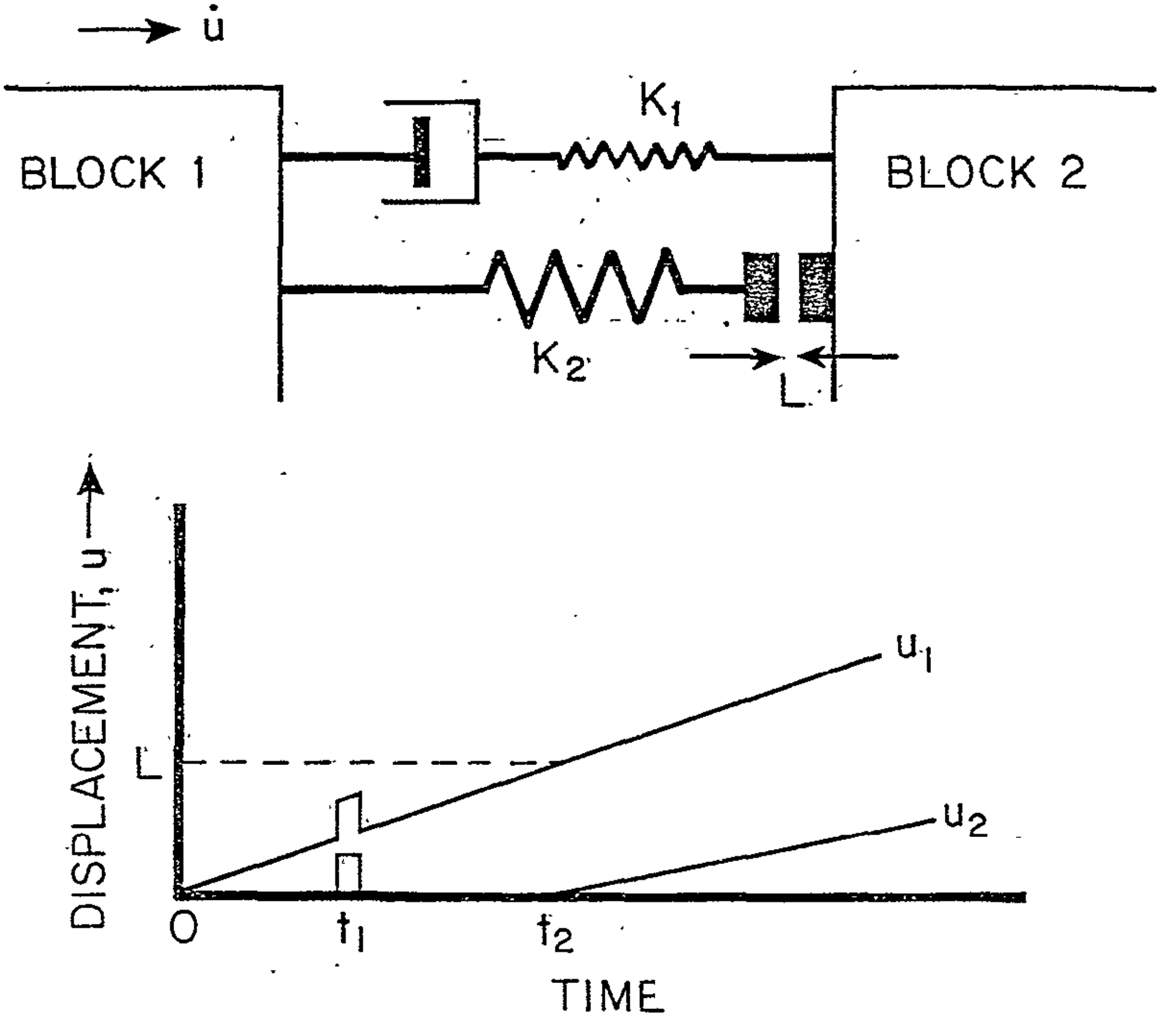

Figure 7